ANL-76-81

ANL-76-81

HIGH-PERFORMANCE BATTERIES FOR PEAK-POWER ENERGY STORAGE AND ELECTRIC-VEHICLE PROPULSION

Status Report for the Period
January 1975

Distribution Category:
Energy Storage—Electrochemical
(UC-94c)

ANL-76-81

ARGONNE NATIONAL LABORATORY
9700 South Cass Avenue
Argonne, Illinois 60439

HIGH-PERFORMANCE BATTERIES FOR OFF-PEAK ENERGY STORAGE AND ELECTRIC-VEHICLE PROPULSION

Progress Report for the Period
April—June 1976

P. A. Nelson	Director, Energy Storage
N. P. Yao	Associate Director, Energy Storage
C. R. Luartes	Assistant Director, Energy Storage
A. A. Chilenskas	Manager, Battery Commercialization
E. C. Gay	Section Manager, Battery Engineering
R. K. Steunenberg	Section Manager, Advanced Electrochemical Technology
J. E. Battles	Group Leader, Materials Development
F. Hornstra	Group Leader, Battery Charging Systems
W. E. Miller	Group Leader, Industrial Cell and Battery Testing
M. F. Roche	Group Leader, Cell Chemistry
H. Shimotake	Group Leader, Cell Development and Engineering
W. J. Walsh	Group Leader, Advanced Engineering

July 1976

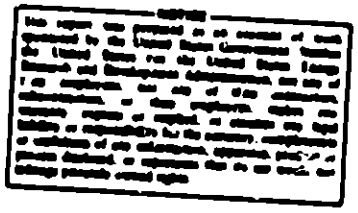

Previous Reports in this Series

ANL-75-1 July—December 1974
ANL-75-36 January—June 1975
ANL-76-9 July—December 1975
ANL-76-35 January—March 1976

FOREWORD

Argonne National Laboratory's program on high-temperature secondary batteries is carried out principally in the Chemical Engineering Division, with assistance on specific problems being given by the Materials Science Division and, from time to time, by other Argonne divisions. The individual efforts of many scientists and technicians are essential to the success of the program, and recognition of these efforts is reflected in the individual contributions cited throughout the report.

TABLE OF CONTENTS

TABLE OF CONTENTS (cont'd)

LIST OF FIGURES

LIST OF TABLES

HIGH-PERFORMANCE BATTERIES FOR OFF-PEAK ENERGY STORAGE AND ELECTRIC-VEHICLE PROPULSION

Progress Report for the Period
April-June 1976

ABSTRACT

This report describes the research and management efforts of the program at Argonne National Laboratory (ANL) on lithium/metal sulfide batteries during the period April-June 1976. These batteries are being developed for energy storage on utility networks and for electric-vehicle propulsion. The present cells, which operate at 400-450°C, are vertically oriented, prismatic cells with a central positive electrode of FeS or FeS_2, two facing negative electrodes of lithium-aluminum alloy, and an electrolyte of molten LiCl-KCl.

Electrodes and cells are being fabricated by several industrial firms under contracts with ANL. These firms are also participating in development of fabrication methods that are amenable to mass production. Cells produced under the first contracts are being tested and evaluated--as single cells and as two- and three-cell batteries. New electrode and cell designs are being developed and tested at ANL, and promising designs will be incorporated in the industrially fabricated cells. The concepts receiving major attention include the fabrication of electrodes in the uncharged state (positive electrodes of Li_2S and Fe and negative electrodes of porous aluminum), the use of carbon-bonded current-collector structures in the positive electrode, the fabrication of electrodes by hot-pressing active materials and electrolyte, and the use of additives to improve electrode and cell performance. In cooperation with industrial firms, efforts are also under way to develop improved cell feedthroughs and electrode separators.

Design work is in progress on a 30-kW-hr battery for a small four-passenger vehicle; this effort includes design calculations and setting specifications for the vehicle. Other battery engineering work is directed to the development of monitoring and cycling equipment and battery components.

Cell chemistry studies in support of electrode and cell development include the wetting of materials by molten LiCl-KCl and potentiometric measurements on metal sulfide phases. Work is continuing on the development of alternative secondary cell systems with calcium-, magnesium-, or sodium-based negative electrodes.

SUMMARY

Cell Fabrication

Development and Testing of Contractor-Produced Cells. The Li-Al/FeS and Li-Al/FeS_2 cells being designed and fabricated by Eagle-Picher Industries, Inc. employ cold-pressed active powders in honeycomb current-collector structures. As a result of testing the first cells, certain design changes were made to accommodate swelling forces within the electrodes and thus avoid early failure due to shorting. These changes were incorporated in the remainder of the cells delivered under their first contract. Four FeS cells (capacity ~150 A-hr; weight, ~2 kg) of the improved design have been tested for periods from 194 to 685 hr. The cells showed similar performance, with ampere-hour efficiencies of ≥99% and watt-hour efficiencies of about 82%. The specific energies at the 10-hr rate were ~60 W-hr/kg and the peak specific powers were ~30 W/kg. The cells are now being used in multicell battery tests. Two Eagle-Picher FeS_2 cells incorporating heliarc spot-welded joints between the positive terminal and the electrode tab, both of which are molybdenum, have been tested for about 500 hr with no joint failures. Preliminary results indicate specific energies of 75 W-hr/kg at the 10-hr rate.

Macroporous, Bonded Positive Electrodes. Carbon-bonded positive electrodes being tested in 12.7 by 12.7 cm prismatic cells have exhibited very good power capability. Low cell resistances (3.8 mΩ for FeS and 5.8 mΩ for FeS_2) have resulted in high peak power densities of 0.55 W/cm^2 for both types of cells. Cell KK-5, an uncharged FeS-Cu_2S cell, has achieved very good sulfide utilizations at high discharge rates: 75% at the 5-hr rate and 63% at the 2-hr rate. This cell has been in operation for more than 1700 hr and 90 cycles and continues to show stable performance. A new type of positive electrode, which incorporates a metallic current-collecting network into the carbon-bonded structure has been developed and will soon be evaluated in cell tests.

Cell Lifetime and Cycle Life Testing. Four 7.6 by 12.7 cm prismatic cells with relatively stable performances are presently being operated in the lifetime studies. Cell S-82, a charged, unsealed Li-Al/FeS_2-CoS_2 cell has been in operation for almost a year (8110 hr, 355 cycles). This cell is presently being used to study problems associated with leakage of particulates from electrodes and their effect on electrode separators. Cells S-86 and S-87, both of which are welded Li-Al/FeS_2-CoS_2 cells assembled uncharged, continue to show stable performance. After 360 cycles and 4875 hr of operation, the ampere-hour efficiency of Cell S-86 remains at 90+%, the internal resistance is constant at 7 mΩ, and the capacity has declined by less than 18% (the present capacity is about 57% of theoretical at the 4-hr rate). Cell S-87 has maintained a very high ampere-hour efficiency, 99+%, for 372 cycles and 3360 hr, and the present capacity at 25 mA/cm^2 is about 50% of theoretical. Cell CB-1, an unsealed Li-Al/$CuFeS_2$ cell, assembled in the charged state, has been in operation for 204 cycles and 3240 hr. The cell has attained typical capacities of 68-70 A-hr (45% of theoretical) at 65 mA/cm^2 charge and discharge; the ampere-hour efficiency remains high (~99%).

Development of Multiplate Cells. Two multiplate cells, each having two positive and four negative electrodes, have been constructed and tested. The positive electrodes in both cells were carbon-bonded FeS_2-CoS_2; the negative

electrodes in one cell were hot-pressed Li-Al and, in the other, Li-Al powder in an iron Retimet structure. Initial emphasis is on lowering cell resistance, but the overall effort is directed toward achieving higher specific energies by minimizing cell weight. Cell MP-1 had an internal resistance of 7 mΩ. Cell MP-2, which has been in operation for 40 cycles, has an internal resistance of 6.5 mΩ and a specific energy of about 53 W-hr/kg at the 6-hr rate. Higher specific energies are expected with design improvements that result in more compact cells.

Materials Development

Electrical Feedthrough Development. Several feedthroughs developed by ILC Technology and 3-M Company were evaluated in simulated cell tests. In all cases, premature failure of the feedthroughs occurred because of the combined effects of electrochemical and galvanic corrosion. Optimum conditions were determined for sealing Conax mechanical feedthroughs (1/4 and 5/16 in.). After successfully undergoing a preliminary test for leak-tightness, the Conax-type mechanical feedthrough developed at ANL was further modified, both to improve the method of crimping and to allow the use of the larger diameter conductors.

Electrode Separator Development. Three types of electrode separators successfully completed 1000 hr of in-cell testing. A composite paper of 90 wt % Y_2O_3 fibers and 10 wt % asbestos fibers, a BN felt, and an Y_2O_3 felt prepared by a precursory process gave satisfactory cell performance and retained their integrity. These separator materials will be made available for further evaluation in engineering-scale cells.

Corrosion Studies. Corrosion studies of candidate materials of construction were conducted in FeS_2 + LiCl-KCl and in FeS + LiCl-KCl environments at 450°C. Included in this study was a series of Ni-Cr alloys not previously tested. In the FeS environment the following materials exhibited suitable corrosion resistance: Inconels 617, 625, 706 and 718, Incoloy 825, Hastelloys B and C, Type 304 stainless steel, molybdenum, niobium and nickel. Only molybdenum showed sufficient resistance to the FeS_2 environment. The sulfidation attack on the nickel-base alloys in the FeS_2 environment resulted in an extended alloy-depletion zone and the formation of a multiphased scale.

Postoperative Examination of Cells. Postoperative examinations of Cells R-7 and R-10, two Li-Al/FeS-Cu_2S prismatic cells assembled in the uncharged condition, were conducted. Unusual conditions observed in these cells include copper migration into the separator and significant dimensional changes in the electrodes. Two commercially fabricated cells of the Li-Al/FeS-Cu_2S type, EP-1B1 and EP-1B2, were also examined. The electrical short that had developed in EP-1B2 was caused by the extrusion of FeS into a 0.010-in. gap between the positive-electrode support frame, which is at the negative electrode potential, and the positive-electrode current collector.

Battery Engineering

The design of a 30 kW-hr battery suitable for driving a small, four-passenger vehicle is in progress. The battery will consist of 160 prismatic subcells (13 by 20 cm); adjacent subcells are connected in parallel to form 80 cells that are connected in series within a cylindrical, insulated

enclosure. This design permits more efficient packaging than a design that employs 13 by 13 cm cells, the size now being industrially fabricated.

Experimentally determined values for the internal resistances of Li-Al/FeS_x cells are being compared with values calculated from resistances of individual components. Good agreement between calculated and measured values (less than 20% difference) was obtained for some cells; for others, the differences were as large as 30 to 40%. In the latter cases, it is postulated that the differences result from the increased resistances produced by surface films on some current collector materials. In general, the comparisons show that cell resistances can be calculated with sufficient accuracy to make an important contribution to cell and battery design.

During this period, a major goal was reached when three Li-Al/FeS cells were operated in a series arrangement. The average specific energy for the three cells was about 45 W-hr/kg, with an ampere-hour efficiency of ∿85% and a watt-hour efficiency of ∿80%.

Cell equalization on two- and three-cell Li-Al/FeS batteries is now routinely performed with a four-cell system devised for laboratory use. Preliminary evaluation of the results of equalization indicates a gain of from 14 to 20% in capacity and energy on subsequent cycles. Work is continuing on a six-cell voltage monitor to control charging and equalizing of a six-cell battery.

Industrial Contracts

Gould completed installation of a large glove-box facility which will provide the capability for cell manufacture needed to fulfill their contract. A computer model for generalized cell design is being used at Gould.

Following testing at ANL of the first four cells (two FeS and two FeS_2) fabricated by Eagle-Picher, several design changes were made for the remainder of the cells under the contract. All of the FeS cells were received and are being tested extensively. Half of the FeS_2 were received and, on the basis of cell performance, approval was given for fabrication of the remaining cells.

Because of difficulties in fabricating cast Li-Al negative electrodes, Catalyst Research is fabricating their first few cells with electrodes of Li-Al vibratorily loaded into porous structures. An FeS_2 cell was fabricated in dry air and is now under test.

Facilities for production of BN fiber are being expanded by Carborundum Co. Alternative methods for binding BN fibers to produce paper or felt separators are being investigated. Prototype separators of both Y_2O_3 and BN have been prepared using an asbestos fiber (∿10 wt %) as a binder to improve mechanical strength. Yttria felt appears to be a promising separator material.

A number of other contracts are directed to the development of feedthroughs, insulators, and aluminum electrode structures, as well as to the production of LiCl-KCl eutectic and Li_2S.

Cell Chemistry

A simple procedure consisting of sintering or melting of Li_2S and subsequent metallographic examination was evaluated as a method for determining impurities in the Li_2S. This method appears to be suitable only for grossly contaminated samples. Metallographic examination did, however, prove to be capable of detecting 1 wt % or less Li_2O in Li_2S. The Li_2S-Li_2O phase diagram was found to be a simple eutectic system with a eutectic temperature of about 975°C and composition near a mole ratio of 1:1.

Further studies of the wetting of materials by molten LiCl-KCl electrolyte have shown that yttria felt is readily penetrated by the salt after a period of time. This result was confirmed by wettability tests with a solid sintered plaque of yttria. However, a sintered plaque of yttria-50 wt % magnesia was less readily wet than the yttria alone. Alumina felt showed poor wetting characteristics that were similar to those of boron nitride.

Potentiometric measurements on metal sulfide phases are being performed to obtain thermodynamic data for the engineering design of cells and batteries. Preliminary results from FeS electrodes show Nernstian behavior, but the reaction appears to be more complex than the simple two-electron process that was expected.

Advanced Cell Engineering

Engineering-scale cells are being operated to test design concepts that show promise of improving cell performance. Both charged and uncharged FeS and FeS_2 cells are being studied. Several methods were tested in FeS cells for increasing the negative electrode capacity of uncharged cells. In Cell R-10, the positive electrode contained Li_2S + Li_2C_2 and in Cell R-12, Li_2S + CaC_2; in Cell R-13, $CaCl_2$ was added to the LiCl-KCl electrolyte. The addition of Li_2C_2 produced the largest gain in cell capacity. In an effort to reduce ohmic resistance, the positive electrode of Cell R-14 was pressed at higher pressures and with lower electrolyte fractions; the cell resistance (3.8 mΩ) was the lowest achieved to date for an uncharged FeS cell with hot-pressed electrodes. Cell BB-1, a charged FeS cell with prototype cold-pressed electrodes supplied by Eagle-Picher Industries, Inc., was operated to evaluate the procedure of fabricating electrodes in a dry room instead of an inert-atmosphere glove box; cell performance was stable, and no adverse effects of the air atmosphere could be observed.

The use of Hastelloy B as an alternative for molybdenum as the current collector material for FeS_2 electrodes was evaluated in Cell R-11; the cell showed a very high utilization (>90%) in early cycles, but the high performance was not sustained. Cell R-8, an uncharged FeS_2 cell with hot-pressed electrodes, is still in operation after 2974 hr and 400 cycles. An uncharged, multiple-electrode FeS_2 cell is nearing completion.

Five button-type cells have been tested. These cells employ two electrodes in holders that are pressed against and separated by a boron nitride separator-insulator, thus eliminating the need for a feedthrough. This type of cell has good potential for ease of assembly and low fabrication costs. Four FeS cells, two charged and two uncharged, and one charged FeS_2 cell were

operated. Currently, the major effort in the button-cell work is directed at controlling the movement of electrolyte within the cell; the use of different electrolytes is also being investigated.

A new type of uncharged Li-Al electrode with improved current collection was evaluated. This negative electrode structure consisted of a woven aluminum fabric containing a metallic current collector of copper and copper-coated iron wire. The performance of this electrode was evaluated in Cell JW-12 using a counter electrode of liquid lithium. The Li-Al electrode showed excellent performance characteristics, similar to those of thick electrodes of Li-Al contained in a porous Retimet current collector.

Alternative Secondary Cell Systems

Experiments ranging from cyclic voltammetry and preliminary cell tests through construction and operation of engineering-scale, prismatic cells of 100-200 A-hr capacity are being carried out to develop new secondary cells. The emphasis is on use of inexpensive, abundant materials.

Cyclic voltammetry experiments have demonstrated that the compounds $CaAl_4$ and $CaAl_2$ can be formed and discharged electrochemically in $CaCl_2$-NaCl electrolyte. The emfs at 550°C were, respectively, 1.371 V and 1.415 V *vs.* an (FeS,Fe,CaS) reference electrode. Cyclic voltammetry of LiAl was conducted for comparison with the calcium-aluminum data.

Two $CaMg_2/CaCl_2$-LiCl-KCl/FeS cells of 12 A-hr capacity were operated with different electrolyte compositions: 10 $CaCl_2$-38 LiCl-52 KCl and 31 $CaCl_2$-54.5 LiCl-14.5 KCl (both in mole percent). The cell with the latter electrolyte had very good polarization characteristics and is now being scaled up to the 100 A-hr level (a prismatic cell) for engineering evaluation.

Recent modifications in the design of prismatic cells include the use of a honeycomb structure in both electrodes to prevent slumping of active material, and the use of a porous metal sheet as particle retainer. The design modifications were the result of engineering tests and evaluation of four prismatic $CaAl_2/FeS$ cells.

In preliminary tests, a Na/FeS_2 cell with an electrolyte of 10 mol % NaCl in LiCl-KCl eutectic demonstrated good performance. The cell emf at 420°C was 1.545 V, in good agreement with thermodynamic calculations that assume formation of Na_2S + FeS. The cell, which was limited by the 0.5 A-hr capacity of the FeS_2 electrode, was operated for fifty cycles at 20 mA/cm^2. Utilization of FeS_2 equivalent to $FeS_2 \rightarrow$ FeS was obtained, with no evidence of capacity decline on cycling or dewetting of the negative electrode. Further tests of this system on a larger scale are planned.

I. INTRODUCTION

Lithium-aluminum/metal sulfide batteries are being developed at Argonne National Laboratory (ANL) for use as (1) energy storage devices for load-leveling on electric utilities and (2) power sources for electric automobiles. The development effort on the energy storage battery, which is funded by ERDA, includes cell chemistry studies, materials studies, electrode development, cell development, battery development, and systems studies. The development of the electric-vehicle battery, which is also funded by ERDA, consists of systems design studies and cell and battery development; most of the more basic studies performed under the energy storage battery program are also applicable to the vehicle-propulsion effort.

Our performance goals for off-peak energy storage and electric-vehicle batteries are given in Table I-1. These goals are the same as those given in the preceding report (ANL-76-35), but revisions are presently being made, as a result of our continuing assessment of development efforts. In the long term, the technical goals (specific energy, specific power, and lifetime) must be achieved with a battery that can be mass-produced commercially at the indicated cost.

TABLE I-1. Performance Goals for Lithium-Aluminum/Metal Sulfide Batteries

Battery Goals	Electric Vehicle Propulsion	Off-Peak Energy Storage
Power		
Peak	60 kW[a]	40 MW
Normal	20 kW	10 MW
Voltage, V	140	1000
Specific Energy, W-hr/kg	120-160[b]	80-150[b]
Energy Output	40 kW-hr	100 MW-hr
Discharge Time, hr	2	5
Charge Time, hr	5	5-7
Watt-Hour Efficiency, %	70	80
Cycle Life	1000	3000
Cost of Capacity, $/kW-hr	20-30[c]	20-30[c]
Heat Loss Through Insulation	150 W	100 kW

[a] Based on the power required to accelerate a 1570-kg car from 0 to 50 mph in 15 sec.

[b] Includes cell weight only; insulation and supporting structure for battery would add approximately 20% to the weight.

[c] Includes cost of cells, but not battery structure and insulation.

To accomplish this, contracts have been made with industrial firms to develop and fabricate electrodes and cells, as well as electrode separators, feedthroughs, and battery components. The contractual efforts and the development work at ANL on cell fabrication, materials development, and battery design are coordinated, so that information exchange is rapid and efficient. Cell chemistry studies and advanced cell engineering studies also provide support for the commercial development effort. A small portion of the overall effort is directed toward investigations of promising alternative systems for secondary battery application.

In June 1976, the organization and management structure of the battery program at ANL were changed to allow our program goals to be achieved more readily. The new management structure is given on the title page of this report. Because the organizational changes had not been completed when this report was written, the format of the preceding quarterly report was retained. The format of the next report will reflect the new organizational structure.

II. COMMERCIAL DEVELOPMENT OF Li-Al/METAL SULFIDE BATTERIES

(A. A. Chilenskas, R. O. Ivins*)

A. Cell Fabrication

(E. C. Gay)

Cell fabrication efforts are directed toward developing and evaluating designs and fabrication methods that will lead to the production of cells meeting our goals for battery performance. In this effort, a strong emphasis is placed on suitability for large-volume production. These designs and methods are further developed by industrial firms under contract with ANL, and contractor-produced cells are tested and evaluated at ANL.

1. Development and Testing of Contractor-Produced Cells

(T. O. Cooper, R. C. Elliott, P. F. Eshman, W. E. Miller)

Eagle-Picher Cells. The cells covered by the contract with Eagle-Picher Industries, Inc. have cold-pressed electrodes and are fabricated in a helium-atmosphere glove box. The first four cells (two FeS_2 and two FeS) delivered to ANL were treated as "prototypes," *i.e.*, they were operated to evaluate cell performance. As a result of these tests, certain design deficiencies became obvious, and a number of design modifications were made before the remainder of the cells under the contract were fabricated.

The changes common to both FeS and FeS_2 cells are as follows. Firstly, the active-material loading of the positive electrode was decreased from 204 to 155 A-hr and the amount of electrolyte was increased to give the same electrode thickness as in the previous design. This capacity is now about the same as that of the negative electrode capacity, so that overall cell capacity was not reduced. The resulting positive electrode is more porous and undergoes less swelling during cell operation. Secondly, the composition of the Li-Al alloy was changed from 43 to 48 at. % Li, by using less aluminum (but the same amount of lithium). Again, the dimensions of the electrodes were held constant by replacing the alloy with electrolyte to give an electrolyte volume fraction of 0.14. This change reduces swelling forces in the negative electrode without reducing the capacity. Thirdly, the design of the inner metal frame was changed, as shown in Fig. II-1, to eliminate contact between the positive electrode and the frame edge, which had caused shorting in the prototype FeS cells.

The improved design shown in Fig. II-1 illustrates an important feature of the Eagle-Picher cells. The two halves of the separator close around the positive electrode to insulate the faces and edges of the electrode. To accomplish this, the BN fabric separator is first soaked in a salt-alcohol mixture and the alcohol is driven off; the remaining salt gives a stiff structure to the BN fabric. While the fabric is still wet, it is molded to the form shown in Fig. II-1. This technique has eliminated the need for folding or sewing the separator and has assured good insulating properties around the edges of the positive electrode.

Four 12.7-cm-square FeS charged cells (EP-1B3, -1B4, -1B5, -1B6) of identical design have been tested. The positive electrodes, which are assembled from half-cells 0.63 cm thick, have total capacities of 155 A-hr.

---

*Now with Coal Technology Programs, Energy and Environment, ANL.

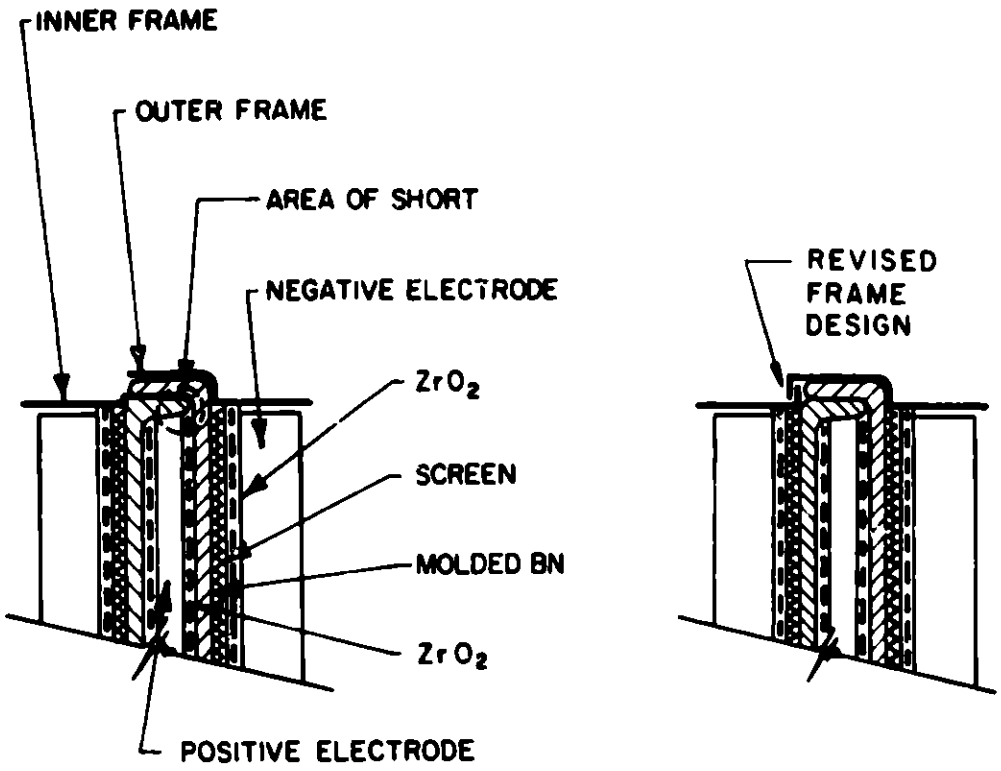

Fig. II-1. Eagle-Picher Cell Designs
a. Design of Prototype Cells
b. Modified Design for Remainder of Cells

The negative electrodes (two per cell) each have thicknesses of 0.72 cm and capacities of 149 A-hr total. The composition of the positive electrodes, in terms of volume fraction, is 0.21 FeS, 0.06 Cu_2S, 0.05 current collector, 0.52 salt, and 0.16 void; that of the negative electrode is 0.63 Li-Al (46 at. % Li), 0.06 current collector, 0.14 salt and 0.17 void. The test periods varied from 685 hr (32 cycles) for Cell EP-1B3 to 194 hr (9 cycles) for Cell EP-1B6. All four tests were terminated voluntarily, with the cells showing good performance; these cells are presently undergoing battery testing (see Section II.C.3).

Cells EP-1B4, -1B5 and -1B6 were operated with mechanical constraints, whereas Cell 1B3 was not. The constraints were metal plates clamped on the major faces of the cell housings to prevent bulging or dimensional changes in the housings that might result from electrode swelling. Cell EP-1B5 was degassed by heating for 24 hr under vacuum before the cell was filled with salt and sealed. The other three cells were not degassed. For this series of identical FeS cells, no marked effect on performance of either cell constraint or degassing was observed.

Cells EP-1B3, -1B4 and -1B5 were tested extensively. The testing procedures were similar to those described in the previous report (ANL-76-35, p. 8). An effort is under way to establish a common testing procedure so that

data acquisition can be standardized and performance results from cells of various designs can be adequately compared. In present tests, cell performance was first stabilized at the 10-hr rate (cycled until the discharge capacity was reproducible). Discharge capacity was then measured at the 5- and 2-hr rates with operation stabilized at the 10-hr rate after each cycle. Charge capacity was measured at the 5-hr rate. Power capability was determined from 15-sec discharge power pulses bracketing the cell's maximum power. These measurements were made at 5 and 50% discharge; after each power pulse the cell was brought back to full charge. The three cells behaved similarly in the tests. Results of some of the tests are discussed below.

Figure II-2 gives typical specific energy data for Cell EP-1B4. The ampere-hour efficiency was >99% and the watt-hour efficiency was >82%. For a charge cutoff voltage of 1.56 V and a discharge cutoff voltage of 1.10 V (IR-included), the specific energies were 60 W-hr/kg at the 10-hr rate and 45 W-hr/kg at the 5-hr rate. These values met expectations for these first contractor-produced cells. A steep decline in capacity occurred with increasing current density. This decline is associated in part with the high series resistance of the cells in this design (about 8.3 to 9.2 mΩ) and with the use of a constant discharge cutoff of 1.1 V. Part of this problem will be alleviated in future cells by development of an improved separator that makes particle retainers unnecessary and by improvement in the distribution of current collector. The peak specific powers for these FeS cells were about 30 W/kg (at 5% discharge and at a current density of about 0.3 A/cm^2).

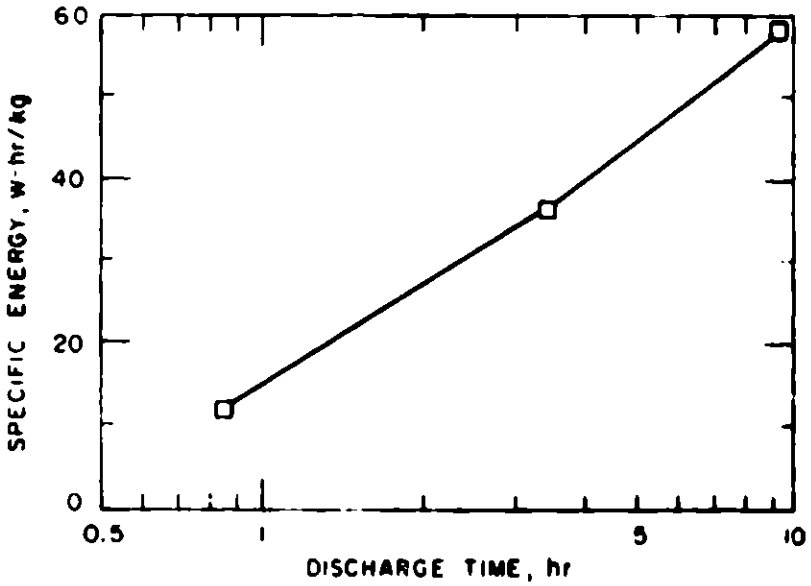

Fig. II-2. Specific Energy of Cell EP-1B4

Figure II-3 shows typical data for the average voltage of each cycle for Cell EP-1B3. The average of these voltages is 1.45 V for charge and 1.20 V for discharge.

Equations for calculating cell power were developed from cell test data (a model and the equations were described in ANL-76-35, p. 10). One

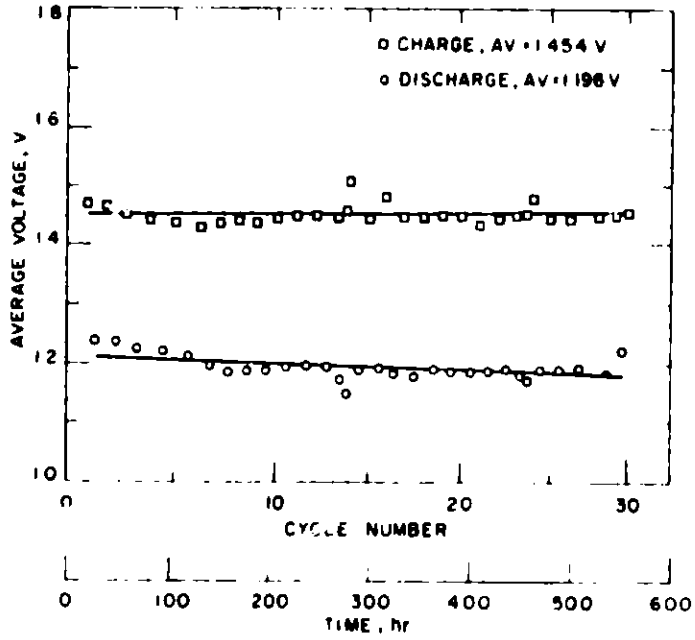

Fig. II-3. Average Voltages for Cell EP-1B3

interesting result was that when the cells were operated at 460°C instead of 435°C, the power output decreased. This decrease results from an increased internal cell resistance, probably owing to an increase in the resistance of the metallic current collector circuit.

As reported previously (ANL-76-35, p. 9), two prototype FeS_2 cells from Eagle-Picher were also tested. In both cells, the connection between the positive electrode tab (molybdenum) and the terminal rod (molybdenum) failed because molybdenum in the weld area recrystallized, and the embrittled metal fractured under stress. Because of the production schedule of parts for the cells, all of the FeS_2 electrodes for the Eagle-Picher cells had been pressed before the problem with the molybdenum connection had become apparent. Therefore, a change in electrode design to accommodate a redesign of this connection was not an available option, and an alternative welding technique was devised. As reported in ANL-76-35, p. 10, the rod diameter in the joint area was increased from 3/16 to 1/4 in., high-temperature grade molybdenum was substituted for regular molybdenum as the rod material,* and the joint was made by heliarc spot-welding. The welded joint is shown in Fig. II-4.

In tests of these joints, the bulk of the rod (the part that was farther than ~0.2 cm from the weld zone) remained ductile. The part of the tab sheet that was held tightly within the slot of the rod showed some recrystallization and embrittlement; however, the tab sheet remained ductile at the rod perimeter, where the stress on the sheet occurs. Joints made in this manner were bent 30° in the weld area before rupturing, thereby indicating sufficient retention of ductility in the joint area. Metallographic studies also indicated the presence of a large, unrecrystallized zone. Retention of ductility in the joint is attributed to the use of HT molybdenum and to the larger joint.

*The use of HT molybdenum was recommended by K. M. Myles of the Materials Development Group.

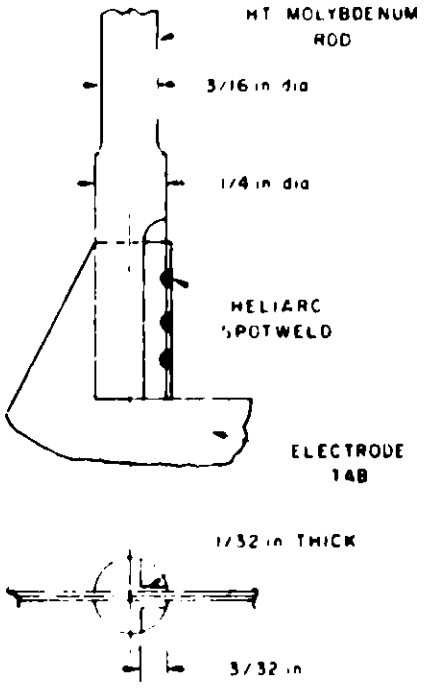

Fig. II-4.

Welded Joint between Molybdenum Terminal Rod and Electrode Tab

Two Eagle-Picher FeS_2 cells that incorporate the molybdenum joint described above have now been operated a total of 500 hr with no failure of the joint. Performance data for these cells are now being obtained, and preliminary results indicate a specific energy of about 75 W-hr/kg at the 10-hr rate. More detailed results will be given in the next report.

2. Macroporous, Bonded Positive Electrodes
(T. D. Kaun)

As previously reported (ANL-76-35, p. 13), the carbon-bonding fabrication method for positive electrodes has been successfully applied to both charged and uncharged FeS and FeS_2 cells. This fabrication method is simple, reproducible, and low in cost. Cells with carbon-bonded electrodes have demonstrated low resistances, namely, 3.8 mΩ for FeS-type cells with iron current collectors and 5.8 mΩ for FeS_2-type cells with molybdenum current collectors. With these low resistances, high peak power densities of 0.55 W/cm^2 have been achieved for both types of cells. The main goal in the development of carbon-bonded positive electrodes is to combine high energy and high power capability in a single cell design.

The physical characteristics and operating data for three 12.5 by 12.5 cm sealed cells with carbon-bonded positive electrodes are shown in Table II-1. In the three cells, BN fabric was used as the electrode separator, with LiCl-KCl as the electrolyte, and ZrO_2 fabric as the particle retainer at all electrode faces. The cells were all operated at 450°C. After 2100 hr, Cell KK-4, a charged FeS_2 cell operated on the upper voltage plateau, started a gradual decline in capacity from the design value of 90 A-hr. Its present capacity is 70 A-hr after 2500 hr and 125 cycles; its coulombic efficiency remains near 100%, with stable average discharge voltage.

Table II-1. Performance of Cells with Carbon-Bonded Electrodes

	Cell KK-4	Cell KK-5	Cell KK-6
Type of Cell	Upper-plateau, FeS_2 charged	FeS uncharged	FeS_2-CoS_2 uncharged
Positive Electrode			
Composition[a]	FeS_2(85), CoS_2(15)	Li_2S(100), Fe, Cu	Li_2S(70), Fe, CoS_2(30)
Half thickness, cm	0.3	0.45	0.5
Theor. Cap., A-hr	180[b]	120	150
Negative Electrodes			
Composition	Hot-pressed Li-Al	Al wire, hot-pressed Li-Al	Cast Li-Al (32 at. % Li)
Thickness, cm	0.6	0.7	0.8
Total Theor. Cap., A-hr	150	180	200
Performance			
Hours	>2500	1750	>400
Cycles	>125	90	>50
Capacity, A-hr	70	90	>60
A-hr Eff., %	99+	86	-
W-hr Eff., %	83	67	-
Resistance, mΩ	5.8	3.8	-
Peak Spec. Power, W/kg	90	85	-

[a]Values in parentheses represent the percent of theoretical capacity supplied by each constituent.

[b]Design capacity 90 A-hr for upper-plateau operation.

Cell KK-5, an uncharged FeS cell, demonstrated very good utilization of the FeS electrode for high discharge rates, namely, 75% at the 5-hr discharge rate (55 mA/cm^2) and 63% at the 2-hr rate (135 mA/cm^2). After 1750 hr, operation of the constrained cell was terminated voluntarily so that the electrodes could be examined. Contrary to the usual behavior, the positive electrode showed no swelling, but the Li-Al negative electrodes, which contained 30 vol % electrolyte in the uncharged state, swelled slightly. The negative electrodes appeared to make good contact with the cell housing, and this may have contributed to the low cell resistance of 3.8 mΩ. Reassembly of the cell and resumption of operation is planned.

Cell KK-6 was operated to test an uncharged FeS_2-CoS_2 electrode versus partially charged Li-Al cast plates (containing 32 at. % Li). The charging of additional lithium into the Li-Al plates has been extremely slow, with cell capacity increasing about 1 A-hr per cycle. The positive electrode contains CoS_2 equivalent to 30% of the electrode capacity. This increase in CoS_2 content over that of past cells is expected to further reduce cell resistance and increase electrode utilization at high discharge rates.

Peak specific powers of cells having carbon-bonded positive electrodes have been among the highest attained by Li-Al/metal sulfide cells. In 15-sec power-pulse tests, Cell KK-5, an uncharged FeS cell, attained a

specific power of >85 W/kg at full charge and 54 W/kg at 50% discharge. Table II-2 compares the best specific powers achieved by various types of iron sulfide electrodes. All cells had electrochemically formed Li-Al negative electrodes except KK-4 (hot-pressed Li-Al) and EP-1B2 (cold-pressed). The low specific power of EP-1B2 may be attributable to the relatively high cell resistance resulting from the design of the positive-electrode lead.

Table II-2. Specific Power Achieved with Iron Sulfide Electrodes[a]

Cell No.[b]	Positive Electrode Type	Fabrication Technique	Positive Electrode Thickness, cm	State of Discharge, %	Specific Power[c] W/kg	Specific Power[c] W/cm^3
S-86	Two plateau, uncharged FeS_2	Vibratory loading	0.63	0	452	1.57
				75	209	0.72
KK-3	Upper plateau, uncharged FeS_2	Carbon-bonding	0.7	0	466	1.29
				50	279	0.77
KK-4	Upper plateau, charged FeS_2	Carbon-bonding	0.6	0	416	1.72
KK-5	Uncharged FeS	Carbon-bonding	0.9	0	355	1.19
				50	223	0.74
R-2	Two plateau, uncharged FeS_2	Hot-pressing	0.56	0	456	1.42
				75	260	0.81
R-7	Uncharged FeS	Hot-pressing	1.2	0	267	0.83
				38	139	0.43
EP-1B2	Charged FeS	Cold-pressing	1.3	0	103	0.31
				50	70	0.21

[a]Specific power based on the weight and volume of the positive electrode, including active material, electrolyte, and current collector.

[b]All cells had one central positive and two negative electrodes; electrode areas were 170 to 320 cm^2; pressed Li-Al electrodes were used in Cell 1B2 and Cell KK-4; electrochemically formed Li-Al electrodes were used in the remaining cells.

[c]15-sec power pulses for Cell EP-1B2 and all KK series cells; 10-sec power pulses for the remaining cells.

A new type of positive-electrode structure, which may also reduce cell resistance, incorporates a metallic current-collector network into the carbon-bonded structure. A modified carbon-bonding paste containing finely divided active material is spread into metal Retimet structures to fill them completely. In the completed structure, active material is carbon-bonded to the Retimet and also to other active material particles. Iron Retimet is used for FeS electrodes and a recently procured molybdenum-alloy Retimet is used

for FeS_2. To evaluate this method, sample structures with 4-mm-thick current collectors were prepared and cured; photomicrographs showed a sufficiently homogeneous distribution of -100 mesh FeS_2 particles within the Retimet structure. The loading was 1.2 A-hr/cm^3 with approximately 60% void volume. This new type of electrode will be tested in a cell now under construction; the active material in the positive electrode is FeS_2 and the current collector is molybdenum-alloy Retimet.

3. Cell Lifetime and Cycle Life Testing
(F. J. Martino, E. C. Gay)

Of primary importance in the lifetime studies is the achievement of our near-term goal of ∿1000 cycles. The 7.6 by 12.7 cm prismatic cells presently being tested have positive electrodes in which the active material was either vibratorily loaded into vitreous carbon foam or bonded to a porous carbon matrix. Presently, four cells are in operation, each achieving relatively stable performance at the 5-hr charge-discharge rates prescribed for the near-term goals.

Cell S-82, an unsealed cell with a positive electrode of FeS_2-CoS_2 in vitreous carbon foam and negative electrodes of Li-Al in iron Retimet, has been in operation for almost a year (8110 hr, 355 cycles). The cell is now being cycled at a current density of 50 mA/cm^2. As discussed later, the cell is presently being used to investigate problems associated with particulate active material that is not contained within the electrodes.

Cells S-86 and S-87, both of which are welded, compact FeS_2 cells, were assembled uncharged (FeS_2-CoS_2 in vitreous carbon foam and aluminum wire plaques). After 360 cycles and 4875 hr of operation, Cell S-86 has an ampere-hour efficiency of 90+% and a constant internal resistance of 7 mΩ. Noteworthy is the less than 18% loss in capacity that has occurred between its typical high capacity and its present capacity of 33 A-hr (57% of theoretical) at a 4-hr rate of 50 mA/cm^2. Cell S-87 has a high ampere-hour efficiency of 99+% after 372 cycles and 3360 hr. Its present capacity at 25 mA/cm^2 charge and discharge is 22 A-hr (49% of theoretical).

Cell CB-1, which has carbon-bonded $CuFeS_2$ and hot-pressed Li-Al electrodes, is performing well. The cell, which was assembled in the charged state, has attained typical capacities of 68-70 A-hr (45% of theoretical) at 65 mA/cm^2 charge and discharge. During the 204 cycles and 3240 hr of cell operation, ampere-hour and watt-hour efficiencies of 98+ and 75%, respectively, have been consistently obtained.

One of the parameters being investigated is the retention of active materials in both the positive and negative electrodes through the use of ZrO_2 fabric. Virtually all test cells without retainers of ZrO_2 have demonstrated poor lifetime characteristics. Cell S-82, which does not employ a retainer cloth in either electrode, had begun to show signs of declining performance after 5600 hr and 202 cycles of operation. In an attempt to alleviate this problem, the BN cloth separator was replaced and the electrolyte was filtered to remove particulates. When the cell was restarted with the new separator, an immediate, marked improvement in performance occurred: the ampere-hour efficiency increased from 50 to 98+% and the capacity from 97 to 132 A-hr (from 50 to 69% of theoretical). These data strongly suggest that the decline

in performance resulted from shorting, since there appeared to be no permanent loss in cell capacity. Development of improved separators (see Section II.B, below) should eliminate the problems associated with containment of active materials within the electrodes.

An important factor in achieving long lifetimes in FeS_2 cells is the structural strength of the electrical connection between the positive-electrode current collector and terminal. These components are usually molybdenum, which has good corrosion resistance but is difficult to weld (see Section II.A.1, above). Accordingly, alternative materials that can be welded more easily are being sought. Cell S-86 employed nickel components with a welded joint that had a resistance of 7 mΩ, whereas Cell S-87 employed a nickel terminal and Hastelloy B current collector with a welded joint of 12 mΩ resistance. Two multiplate cells, discussed below, have welded connections between nickel terminals and molybdenum current collectors. These welds have adequate structural strength and resistances of about 7 mΩ. To date, cell performance data have not indicated any problems with these connections. The nickel-molybdenum welded connections are of particular interest and will be tested further in FeS_2 cells.

4. Development of Multiplate Cells
(F. J. Martino, E. C. Gay)

A multiplate cell design is being investigated in an effort to achieve higher specific energy in compact cells. In the initial studies, emphasis is on lowering cell resistance; in succeeding cells, effort will be directed toward minimizing cell weight and achieving higher specific energy.

Cell MP-1, an upper-plateau cell, had two positive carbon-bonded FeS_2-CoS electrodes and four hot-pressed Li-Al electrodes and a weight of 1.9 kg. Connections between the positive nickel terminals and the molybdenum current collectors were made by welding. The negative electrodes utilize a series of "shelf-like" ridges of iron mesh for improved current collection. All electrodes have particle retainers of zirconia fabric. During 50 cycles and 500 hr of cell operation (terminated because of a leak in the housing), typical capacities were ~58 A-hr, corresponding to 50% utilization at 10 A (25 mA/cm^2) charge and discharge. Cutoff voltages of 1.07 and 1.99 V (IR-free) were maintained and throughout operation the internal resistance was constant at 7 mΩ. The average specific energy was 45 W-hr/kg at charge and discharge rates of about 5 hr.

In the design and construction of Cell MP-2 (two-plateau FeS_2-CoS_2/Li-Al, 7.4 by 12.6 cm), an attempt was made to minimize component weights and to provide space for electrode expansion within the cell housing. This was done by reducing the positive electrode capacity to allow for more electrolyte (initially 60 vol % instead of 41 vol %) and providing more void volume for expansion. The positive electrodes were thin (12 mm) and molybdenum wire was woven within the molybdenum current collector to provide better current collection with a lower internal resistance; again, a satisfactory weld to the nickel terminal was made. The negative electrodes were Li-Al in iron Retimet; these structures were then cold-pressed to produce a structure with a void volume of 34%. Although individual component weights were reduced, the total cell weight was not reduced significantly from that of Cell MP-1 because the amount of electrolyte was increased.

The performance of Cell MP-2 has not yet stabilized, but after 40 cycles and 435 hr of operation, the capacity is 68 A-hr (corresponding to 57% utilization) at 7.0 A (20 mA/cm^2) charge and discharge rates. Cutoff voltages of 1.04 and 1.9 V (IR-free) are being maintained, and the internal resistance is stable at 6.5 mΩ. To date, Cell MP-2 has achieved a specific energy of 53 W-hr/kg (at about the 6-hr rate); this value is expected to improve as operation continues.

Future work on multiplate cells will include testing of materials that can serve as both separators and particle retainers, as well as development of larger-scale cells (12.7 by 17.8 cm).

B. Materials Development
(J. E. Battles)

Efforts in the materials program are directed toward the development of various cell components (*e.g.*, electrical feedthroughs, electrode separators and current collectors, and cell hardware), corrosion testing of candidate materials for these components, and postoperative examination of cells to evaluate the behavior of the various construction materials as well as the behavior of the lithium-aluminum and metal sulfide electrodes.

1. Electrical Feedthrough Development
(K. M. Myles, J. L. Settle)

The corrosive environment within Li-Al/LiCl-KCl/FeS_x cells precludes the ready adaptation of most commercially available electrical feedthroughs. The few that are compatible with the cell environment employ mechanical seals. At present, these feedthroughs are unacceptably bulky, and their seals lack sufficient leak-tightness. Accordingly, new and innovative brazed seals are being sought and, at the same time, work is in progress to minimize the shortcomings of the mechanical seals.

Both ILC Technology and 3-M Company have produced brazed-type feedthroughs as a result of development contracts with ANL (see Section II.D). The feedthroughs were subjected to simulated cell tests to evaluate their expected lifetimes. In all cases, the feedthroughs failed even at low cutoff potentials in relatively short times owing to the combined effects of electrochemical and galvanic corrosion. The test results are presently being assessed by the two firms.

A systematic study was undertaken to determine the optimum conditions for sealing 1/4- and 5/16-in. Conax-type mechanical feedthroughs, which will be required for future use with larger commercial cells. Variables such as the amount of BN powder sealant, its particle size distribution, and the ultimate load-bearing capacity of the ceramic insulators (BN, Y_2O_3, Al_2O_3, and BeO) were evaluated by measuring the static leak rate through the assembled feedthroughs. Leak rates as low as 7×10^{-7} cm^3(STP) air/sec were achieved. The Conax feedthrough modified at ANL was also evaluated and proved to have an acceptably low leak rate. An effort is also under way to enlarge this feedthrough for use with larger diameter conductors and to improve the method of crimping the upper portion of the housing. Solder glasses will be evaluated as secondary sealants (outside the primary BN powder seal) now that the leak rates are acceptably low.

2. Electrode Separator Development
(J. P. Mathers, T. W. Olszanski)

Paper and felt electrode separators are being developed as alternatives for the BN fabric which is currently used in Li-Al/KCl-LiCl/FeS_x cells. The paper and felt separators are expected to be considerably less expensive than the BN fabric and to provide more effective particle retention within the electrodes.

Three promising paper and felt materials have successfully undergone in-cell testing for a period of 1000 hr. The first material was a composite paper of 90 wt % Y_2O_3 fibers and 10 wt % asbestos fibers, developed at the University of Florida.* The asbestos provides the needed strength for handling and cell assembly; however, it is not stable in the cell environment. Therefore, to maintain the structure of this paper in an operating cell, the paper must be maintained in a state of compression between the electrodes. The second material was a BN felt (C715-94), developed by the Carborundum Company,** in which BN fibers were bonded together with a BN binder. The third material was an Y_2O_3 felt developed by Zircar Products, Inc. It was prepared by a precursory process in which fibers of a rayon felt were impregnated with YCl_3 and then converted to fibers of Y_2O_3 by controlled pyrolysis. The resulting felt, consisting of mechanically interlocked Y_2O_3 fibers, required no binders.

These three materials were characterized by various physical and mechanical property measurements, which are presented in Table II-3. On the basis of these results, all three were judged suitable for in-cell testing; however, the Y_2O_3 felt appears to have the best combination of properties for use in practical cells. Each of the paper and felt separators was tested in a Li-Al/LiCl-KCl/FeS cell of a design that has been described previously (ANL-76-35, pp. 19-21). The cells were cycled continuously at a current density of 76 mA/cm^2 and a temperature of 450°C. All three cells showed satisfactory electrical performance and were operated for a period of 1000 hr before being terminated voluntarily.

Postoperative examination of the cells showed that in each case the upper electrode cup had ruptured. This cup contained FeS in one of the cells and Li-Al in the other two cells. Excessive expansion of the active materials caused the rupture in each case.

The integrity of the Y_2O_3-asbestos separator was maintained fairly well, although some void areas were observed. The cause of these voids has not been determined. Examination by scanning electron microscopy (SEM) showed no apparent signs of attack of the Y_2O_3 fibers, but the asbestos was destroyed, as had been expected. The BN felt and Y_2O_3 felt separators maintained their integrity in the test cells and no voids were observed. Examination by SEM for evidence of attack in the BN and Y_2O_3 felts is in progress.

All three separator materials will be made available for further evaluation in engineering-scale cells.

---

*Professor R. D. Walker and C. C. Cheng, funded by the U.S. Energy Research and Development Administration.

**R. S. Hamilton, Research and Development Division, funded by Argonne National Laboratory.

Table II-3. Properties of Paper and Felt Electrode Separators

Property	Y_2O_3-Asbestos Paper	BN Felt	Y_2O_3 Felt
Thickness, mils	35	72	68
Percent Porosity	79	93	96
Air Resistance,[a] sec/in.	514	1.94	1.09
Burst Strength,[b] psi/in.	23	7	22
Flexibility,[c] in.	1	1	0.25
Wettability[d]	Good	Poor	Fair

[a]Time required for the flow of a standard volume of air through the separator, divided by separator thickness.

[b]Hydrostatic pressure required to rupture the separator, divided by separator thickness.

[c]Diameter of the smallest cylindrical mandrel around which the separator can be bent without tearing.

[d]Ease with which the separator can be impregnated with molten LiCl-KCl electrolyte.

3. Corrosion Studies

(J. A. Smaga, J. E. Battles)

Corrosion studies were completed on a series of Ni-Cr alloys not previously tested. Hastelloys B and C and Type 304 stainless steel were also included in this study, as were molybdenum, niobium, nickel, and Armco electromagnet iron. All of these materials were evaluated in equal volume mixtures of both FeS_2 + LiCl-KCl and FeS + LiCl-KCl, with the exception of Armco iron which was tested in the FeS environment only. The tests employed time intervals of 500 and 1000 hr and a temperature of 450°C. The nominal compositions of the alloys and a summary of the test results are given in Table II-4.

The FeS corrosion study indicated that all of the materials evaluated, with the exception of Armco iron, have acceptable corrosion resistance at 450°C (the corrosion rates were considerably lower than the value of 80 μm/yr or less that is considered acceptable corrosion resistance). Iron-rich intermetallic reaction layers were formed on the niobium samples, and the niobium was embrittled (similar results had been obtained in tests at 500°C, see ANL-76-9, pp. 46-49). The nickel samples also reacted to form iron-rich intermetallic layers. The corrosion rates of molybdenum and the nickel-base alloys (Inconels, Incoloy, and Hastelloys) were less than 7 μm/yr; however, Inconels 706 and 718 and Hastelloy B exhibited minor intergranular attack, with Inconel 706 showing the most extensive grain-boundary penetration.

In the FeS_2 environment, only molybdenum has the required corrosion resistance. The molybdenum samples showed a slight gain in weight; however,

Table II-4. Results of Corrosion Tests in FeS and FeS_2 Environments at 450°C

Material	Corrosion Rate,[a] μm/yr			
	FeS + LiCl-KCl		FeS_2 + LiCl-KCl	
	500 hr	1000 hr	500 hr	1000 hr
Molybdenum	2.0	4.1	+1.8	+0.20
Niobium	+30	+22	2900	-
Nickel	+17	3.0	>6600	-
Armco Iron	470	450	-	-
Inconel 617 (Ni-22Cr-12.5Co-9Mo-1Al)	1.8	2.7	890	1280
Inconel 625 (Ni-22Cr-9Mo-5Fe-3.6Nb)	1.7	3.6	890	930
Inconel 706 (Ni-36Fe-16Cr-3Nb-1.8Ti)	5.3	3.9	4300	2300
Inconel 718 (Ni-19Cr-18Fe-5Nb-3Mo-0.8Ti-0.5Al)	6.6	3.4	2400	-
Incoloy 825 (Ni-28Fe-22Cr-3Mo-2.2Cu-0.8Ti)	2.2	1.9	3140	-
Hastelloy B (Ni-28Mo-5Fe-1Cr)	1.6	3.4	220	680
Hastelloy C (Ni-17Mo-16Cr-5Fe-4W)	1.5	0.33	370	970
304 SS (Fe-19Cr-10Ni)	4.7	2.2	>5000	-

[a] Numerical values preceded by "+" represent the formation rates of reaction layers. Values preceded by ">" represent corrosion rates based on the initial weight of the sample. A value of ≤80 mμ/yr is considered acceptable.

no evidence was found by metallography or SEM of a surface layer such as MoS_2, which had been observed in tests at 500°C. Niobium, nickel, and Type 304 stainless steel underwent severe attack. Of the new alloys tested, Inconels 617 and 625, which are solid-solution alloys, showed the best resistance to the FeS_2 environment, but their corrosion rates were more than an order of magnitude higher than acceptable. As a group, the solid-solution Hastelloys, which are typically higher in nickel and molybdenum and lower in chromium than the Inconels, had the best resistance of the alloys tested, but their corrosion rates at 450°C were still higher than acceptable.

The sulfide scales observed on the nickel-base alloys exposed to the FeS_2 environment were examined by both scanning electron microprobe* and X-ray diffraction** techniques. These scales consisted of particles of one or more secondary sulfide phases dispersed in NiS or of a solid solution of FeS in NiS if the alloy contained a significant amount of iron. The dispersed phases included Cr_2S_3, $FeCr_2S_4$, Ni_3S_2, CoS, and $NiCoS_4$, depending on the alloy composition. These findings, combined with metallographic examinations, suggest that many aspects of the sulfidation attack in this environment, including the morphology and growth characteristics of the sulfide scale, parallel those reported for binary metal systems in sulfur vapor and H_2S environments.

* Performed by C. A. Seils, Chemical Engineering Division, ANL.

** All X-ray diffraction analyses discussed in this section were performed by B. S. Tani, Analytical Chemistry Laboratory, ANL.

The outward diffusion of certain alloying elements and their subsequent reaction to form the sulfide scales produced zones in the base metal adjacent to the sulfide scale that were porous and were altered in chemical composition. These porous zones were quite deep, for example, up to 180 μm in Inconel 625 samples after 1000 hr. In these zones, the concentrations of such elements as nickel, iron, chromium and cobalt decreased, and, as a result, the concentrations of molybdenum, niobium, and tungsten increased. The concentration changes were gradual and diffusion-controlled, although elements such as aluminum and titanium appeared to concentrate at the metal/sulfide interface.

4. Postoperative Cell Examination
(F. C. Mrazek, K. C. Carroll, J. E. Battles)

Postoperative examinations are conducted on test cells primarily to evaluate the performance of various construction materials, in particular, feedthroughs, current collectors, electrode separators, and cell housings. These postoperative examinations provide important information, not only on the compatibility of cell components with the cell environment, but on the performance and behavior of the lithium-aluminum and metal sulfide electrode materials. The examination procedures were described in a previous semiannual report (ANL-8109, p. 72).

a. Cells Fabricated at ANL

Postoperative cell examinations were completed on prismatic engineering-scale cells R-7 and R-10, which were assembled in the uncharged state and operated at 450°C (Shimotake and Bartholme, ANL-76-35, p. 46). Operation of each cell was terminated because of electrical shorting between the electrodes after 3408 hr (179 cycles) for Cells R-7 and 1732 hr (128 cycles) for Cell R-10. The initial materials in the positive electrodes were Li_2S, iron, and copper powder (R-7) and Li_2S, iron, copper, and Li_2C_2 powder (R-10). In both cells, aluminum wire was the starting negative electrode. The development of initially uncharged cells was undertaken in an effort to prevent excessive swelling and outgassing in cells and to improve the utilization of active materials.[1]

The cross sections of Cells R-7 and R-10 are shown in Fig. II-5, where it is apparent that the swelling was excessive in Cell R-10, a sealed cell (R-7 was not sealed). The thickness of Cell R-7 had increased from 2.7 to 3.5 cm and that of Cell R-10 from 3.0 to 4.6 cm. Figure II-5a shows that a substantial increase also occurred in the length of the negative electrodes of Cell R-10. The negative electrodes in Cell R-7 showed only a small increase in length. Thus, the problem of electrode (cell) swelling has not been prevented by assembling cells in the uncharged condition. Mechanical constraint does prevent cell swelling, but may be the source of other problems (ANL-76-9, p. 52).

Metallographic examination of both cells showed bands of a copper-bearing particulate extending through the ZrO_2 fabric that served as a particulate retainer for the positive electrode and also through the BN electrode separator. The electrical shorting observed in these cells has been attributed to these metallic stringers; no other evidence of specific short circuits could be located. Cutting of the cell into small sections

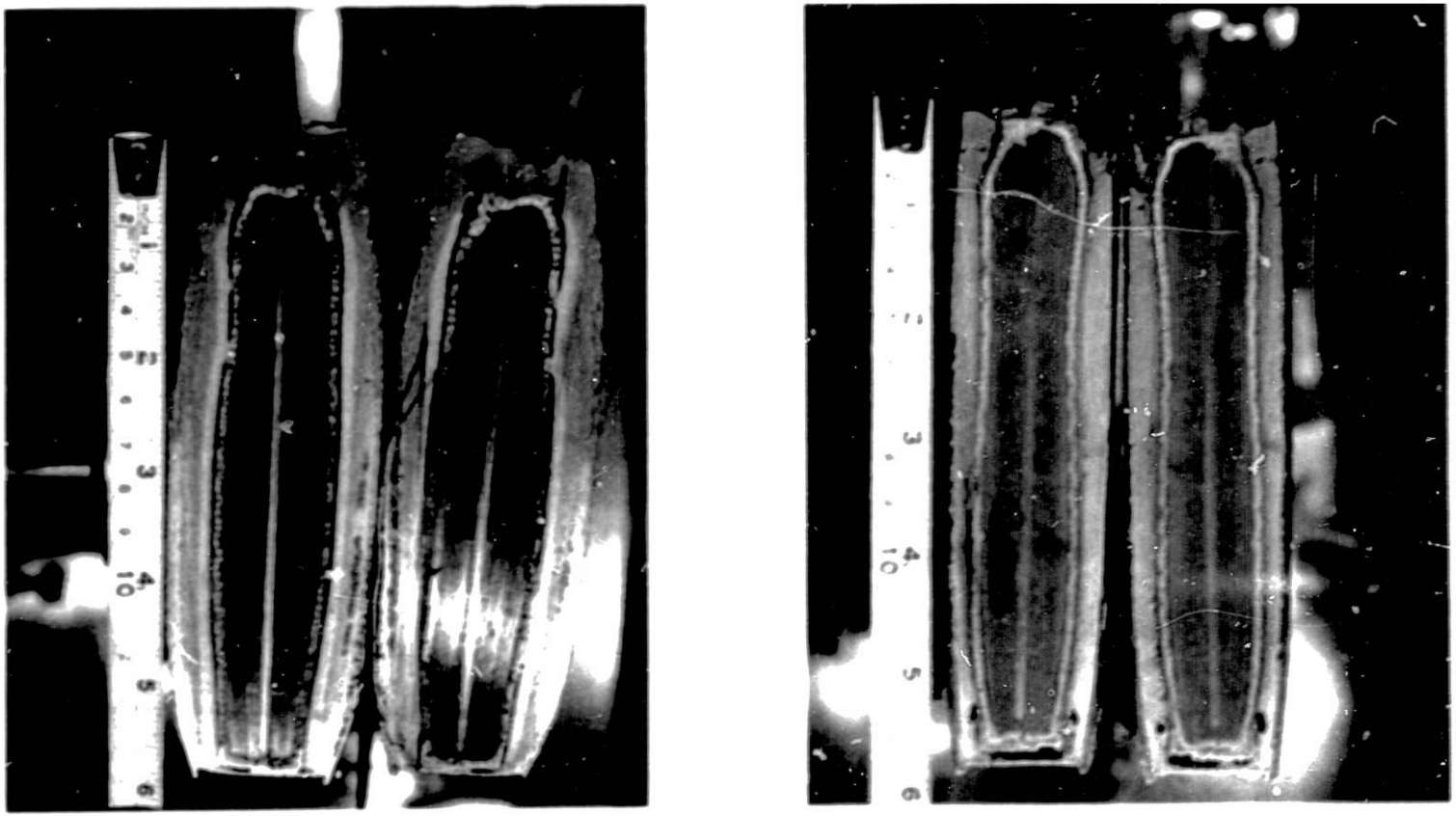

a. Cell R-10

b. Cell R-7

Fig. II-5. Cross Sections of Cells R-10 and R-7 Showing Swelling and Distortion of the Electrodes

yielded only a gradual increase in resistance in the smaller sections, thereby indicating multiple conductive paths. The presence of copper-bearing particulate in the separator is unusual, and the mechanism responsible for it is unknown at this time.

As noted above, the positive electrode of Cell R-10 contained Li_2C_2 as an additive (representing 20 wt % of the active material). Carbon analysis* showed 3.67 and 0.19 wt % carbon in the positive and negative electrodes, respectively. In Cell R-7, which was similar to Cell R-10 except for the addition of Li_2C_2, the carbon analysis showed only 0.07 and 0.02 wt % carbon in the positive and negative electrodes, respectively. The results indicate that a substantial transport of carbon from the positive electrode to the negative electrode occurred in Cell R-10. An important question is how the presence of fine carbon particles might affect the electronic conductance of the electrolyte.

b. Cells Fabricated Under Industrial Contracts

Examinations were also completed on two Li-Al/FeS-Cu_2S cells (EP-1B1 and EP-1B2), which were prismatic engineering-scale cells fabricated by Eagle-Picher Industries, Inc. and tested at ANL. The positive electrodes were FeS plus a Cu_2S additive, the negative electrodes were powdered Li-Al, and in both, iron honeycomb structures served as current collectors. The cell housings were low carbon steel (AISI-1010). Boron nitride electrode separators and ZrO_2 fabric particle retainers were used, along with 325-mesh stainless steel screens. (These cells are called prototypes in Section II.A.1.)

Cell EP-1B2 was operated with mechanical constraints to prevent swelling. A short circuit developed in this cell after 480 hr (22 cycles) of operation at 433°C. Figure II-6a shows a cross section of this cell. Although electrode swelling appears moderate, the negative electrodes are about 25% thicker than the original 0.72 cm. The positive electrode shows only minor swelling in most regions, except for one bulge located 1 cm from the bottom, where the expansion is about 15%. X-ray diffraction analysis of the positive electrode material showed the presence of X_{Cu}-phase (a modified form of Li_2FeS_2, called X-phase), FeS, and α-Fe. The distribution of active material in the negative electrode was determined by a computer scanning method described previously (ANL-75-36, p. 74). The distribution varied from 20 vol % near the positive electrode interface to 63 vol % on the side farthest from the positive electrode. The active material loading was initially 85 vol %. The short circuit in this cell was located near the top of the cell between the positive-electrode support frame, which is at negative electrode potential, and the positive-electrode current collector; in this area FeS had extruded from the positive electrode into the 0.025-cm gap and had caused the short circuit. The constraint applied to minimize the increase in thickness probably contributed to the extrusion of FeS from the electrode.

The other cell, EP-1B1, was sealed and operated for 7 cycles before developing a short circuit. No constraint was employed to prevent electrode swelling. Figure II-6b shows the swelling behavior of Cell 1B1,

*N. L. Johnson and I. M. Fox, Analytical Chemistry Laboratory, ANL.

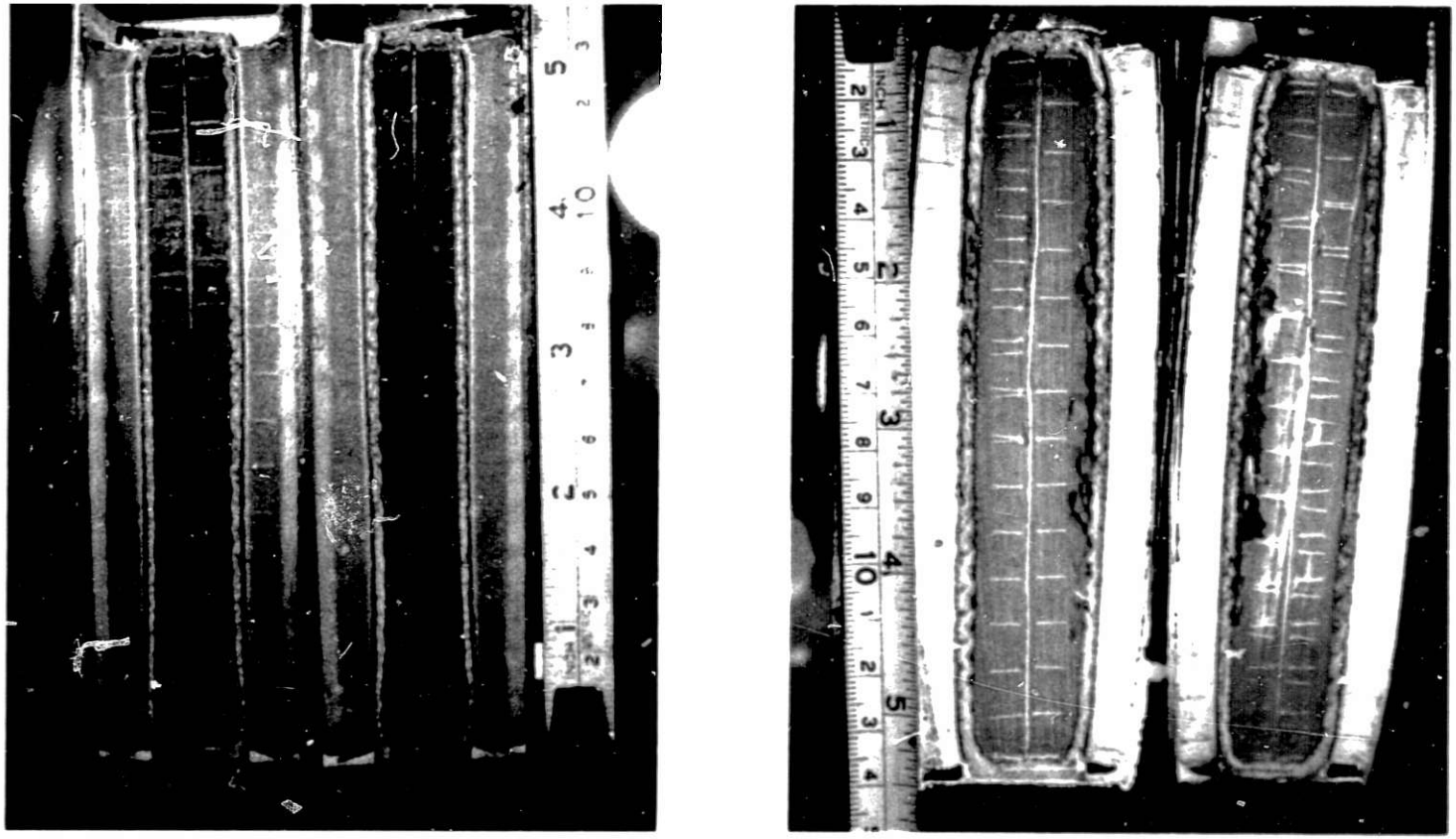

a. Cell EP-1B2

b. Cell EP-1B1

Fig. II-6. Cross Sections of Cells EP-1B2 and EP-1B1 (the lesser extent of swelling in Cell EP-1B2 is attributed to mechanical constraint during operation)

which is quite different from that of Cell EP-1B2. The positive electrode thickness had increased by 30 to 50% from the initial value of 1.27 cm. The negative electrodes appeared to have increased in thickness by an average of 6% from the initial value of 0.72 cm. The nominal loading of Li-Al in these electrodes was 70 vol %. Poor electrolyte penetration of the BN fabric separator made it possible to remove the cloth and probe it for electrical short circuits. The cell resistance of 80 Ω was found to be caused by many conducting paths across the BN cloth. Material from two of these low resistance paths, taken from the negative electrode side and identified by X-ray diffraction as FeS and α-Fe, was presumed to be the source of the short-circuiting across the BN separator.

C. Battery Engineering
(A. A. Chilenskas)

1. Design Studies

a. 30 kW-hr Electric Vehicle Battery
(G. J. Bernstein, A. A. Chilenskas)

A design study has been initiated to assist in the development of an electric-vehicle battery cell that will meet specific goals for an Li-Al/FeS_2 cell fabricated by an industrial firm in 1978. To permit more efficient packaging, the cell size is 13 by 20 cm (the current industrial capability is for 13 by 13 cm cells). The performance goals for industrially fabricated cells for an electric-vehicle battery are shown in Table II-5 for 1976, 1978, and 1981. The specifications and performance goals for an electric automobile are shown in Table II-6; the goals for 1978 and 1981 are based upon the cell performance goals shown in Table II-5 for those years.

Table II-5. Performance Goals for Industrially Fabricated Li-Al/FeS_2 Cells

Goals	1976	1978	1981
Specific Energy,[a] W-hr/kg	75	110	160
Peak Power,[b] W/kg	75	110	200
Energy Efficiency, %	70	72	75
Lifetime[c]			
Deep Discharges[d]	200	400	800
Automobile Cycles	600	1,200	2,400
Equivalent kilometers	32,000	64,000	128,000
Years of Use	2	4	8

[a]At 4-hr discharge rate.

[b]15-sec pulse at 50% discharge.

[c]Lifetime based upon a deep discharge equivalence of 160 km; automobile cycles based upon 5 cycles/week at 32 km/cycle and one cycle/week at 160 km/cycle (16,000 km/yr).

[d]Deep discharge is equivalent to 70% utilization of the active electrode materials.

Table II-6. Vehicle Specifications and Performance Goals

	1978	1981
Test Weight (136-kg load), kg	1272	1272
Cell Weight, kg	300	300
Battery Weight, kg	400	400
Battery Output at Terminals		
Energy, kW-hr at C/4 rate[a]	30	49
Peak Power, kW (15-sec pulse)	29	59
Time to Accelerate, sec		
0-64 km/hr	<15	
0-89 km/hr		<15
Top Speed, km/hr	>97	>129
Driving Range, km		
Residential (SAE J227)	171	254
At Constant Speed		
40 km/hr	600	975
89 km/hr	185	300

[a]Current drawn at a rate that would completely discharge the cell in 4 hr.

A Li-Al/FeS_2 cell (13 by 20 by ~2.5 cm) is the basis for the design of a 30 kW-hr battery for powering a small, four-passenger vehicle. (A 42 kW-hr battery was designed previously, see ANL-76-35, p. 26.) The present battery design has 160 prismatic subcells, 13 by 20 cm, which are arranged in two parallel rows. Adjacent subcells are connected in parallel to form 80 cells that are connected in series.

A cylindrical enclosure, shown in Fig. II-7, has been designed to hold the 400-kg vehicle battery. This enclosure is a double-walled vessel 43 cm in diameter and 244 cm long and is located within a structural cylinder which serves as a supporting element of the vehicle body. Thermal insulation is provided by multifoil insulation within the evacuated double wall and by a thick insulating plug at the front end. The main power leads, the cell charging and equalizing circuit conductors, heater conductors, thermocouples, and air cooling ducts pass through the plug and are sealed to it to maintain a dry, inert atmosphere within the battery enclosure.

A bench-scale version of this enclosure is being procured for testing and the design of an alternative unit is also being undertaken. Primary effort is directed toward the design of a low-cost unit suitable for mass production.

b. Cell Resistance Calculations
(M. A. Slawecki*)

Calculations of cell internal resistances are continuing. Values were calculated for various cells which have been, or are being,

*Chemical Engineering Division, ANL.

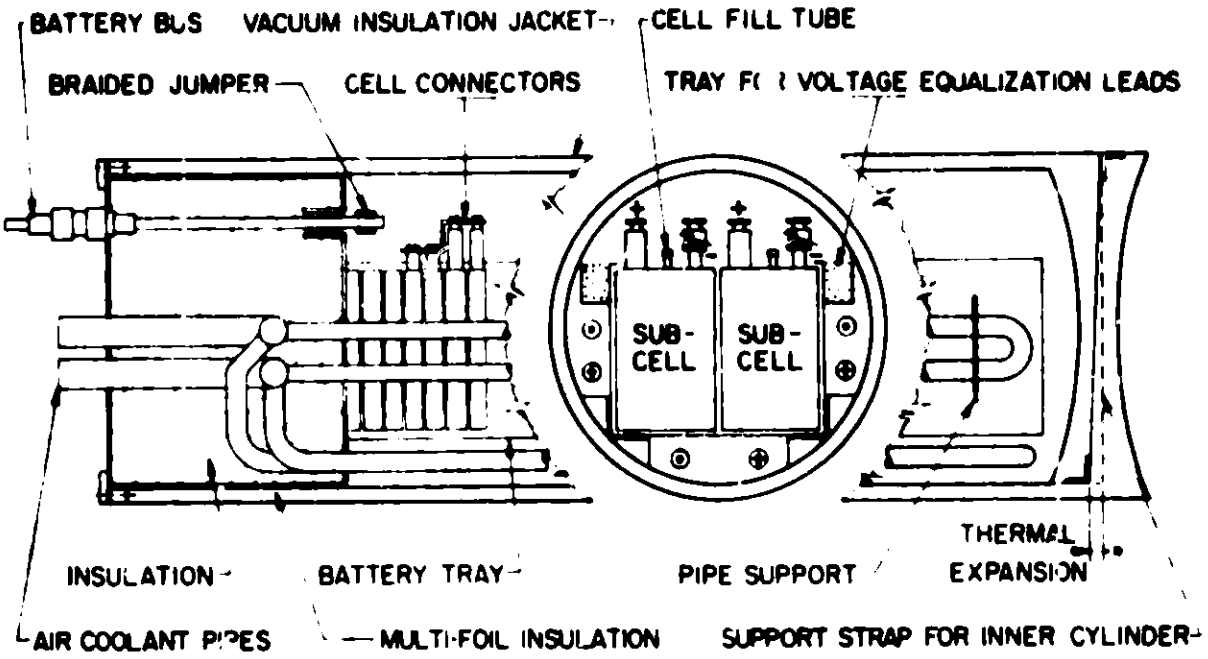

Fig. II-7. 30 kW-hr Electric Vehicle Battery

operated at ANL, and these were compared with measured cell resistances, as shown in Table II-7. The assumption was made in 11 cases that the cell diffusional resistance is twice that of the electrolyte resistance in the fully discharged state and is zero in the fully charged state.

The calculated and measured values for Cells S-86, R-6, R-10, EP-1B3, and 1B/F1 show good agreement, i.e., less than 20% difference, except for the value for Cell R-10 in the fully charged state, where the difference is 25%. The difference between measured and calculated values for Cells S-87 and R-11 which have current collectors and positive terminals of Hastelloy B is between 30 and 40%. Although the calculated resistances for these two cells are higher than those of the other cells owing to the use of Hastelloy B current collectors, the measured values are even higher. This is attributed to a surface film on the Hastelloy B current collector which effectively raises the cell resistance. If this effect exists, the additional resistance should be inversely proportional to the surface area of the current collector. To test this postulate, the resistance for Cell R-11 was recalculated taking into account the difference between the measured and calculated resistance values for Cell S-87 and the difference between the surface areas of the two current collectors. The values (shown in parentheses in Table II-7) are very close to the measured cell resistance of Cell R-11.

Cell R-5 is an FeS cell without a copper additive; the difference between measured and calculated values is attributed to a higher contact resistance between the current collector and the electrode material. The reason for the discrepancy between measured and calculated values for Gould Cell 1-002 and for Cell EP-2B4 is not known. Cell 1-002 did not operate satisfactorily, and it is possible that the higher measured resistance is related to problems with cell design.

Table II-7. Comparison of Measured and Calculated Cell Resistances

Cell No.	Type of Cell[a]	Electrode Area, cm^2		Cell Resistance,[b] mΩ Meas.	Calc.
S-86	FeS_2-CoS_2 (Ni)	194	C	4.4	4.0
			D	7.8	7.7
S-87	FeS_2-CoS_2 (Hast. B)	194	C	13.9	8.4
			D	17.0	12.1
R-5	FeS (Fe)	297	C	5.9	3.7
			D	9.9	6.3
R-6	FeS-Cu_2S (Fe)	297	C	4.0	3.7
			D	6.0	6.3
R-10	FeS-Cu_2S (Fe)	297	C	5.0	3.7
			D	6.5	6.3
R-11	FeS_2-CoS_2 (Hast. B)	297	C	11.6	7.7 (11.2)[c]
			D	15.0	10.2 (13.7)[c]
Gould 1-002	FeS-Cu_2S (Fe)	300	C	12.2[d]	7.4
			D		9.4
EP-1B3	FeS-Cu_2S (Fe)	300	C	8.9	7.6
			D	9.6	10.0
EP-2B4	FeS_2-CoS_2 (Mo)	300	C	8-10.4[d]	4.8
			D		7.2
1B/F1	FeS-Cu_2S (Fe)	300	C	6.4-8.0[d]	7.2
			D		8.9

[a]All cells had Li-Al negative electrodes. All cells had BN separators except 1B/F1, which had Y_2O_3. Parenthetical expressions denote positive electrode current collector material.

[b]C = charged, D = discharged.

[c]Corrected for surface film on Hastelloy B current collector (see text).

[d]Experimental values for fully charged or fully discharged cells not available.

These studies demonstrate that cell resistance values can be calculated with sufficient accuracy to make an important contribution to cell design. Calculations of this type will be continued for other operating cells to verify their usefulness in cell design work.

2. Component Testing
(F. Hornstra, E. C. Berrill, W. W. Lark)

The successful operation of the data-acquisition system and computer-controlled data plotter for the battery laboratory was demonstrated in conjunction with two-cell battery tests. Hard-copy prints of current and voltage as a function of time for single cells and two-cell arrays were obtained. In addition, computer calculations of cell watt-hours and ampere-hours and their

efficiencies were obtained. Work is continuing on expansion of the system to accommodate additional cells, increase the timing resolution, and reduce the interval between data-recording time and the time when the graphic display information is available.

Cell equalization on two- and three-cell Li-Al/FeS batteries is now routinely done with the laboratory system described in the previous quarterly report (ANL-76-35, p. 32). Work is continuing on a voltage monitor to control charging and equalizing of a six-cell battery. Similar in concept to the present four-cell monitor, this new unit is more sophisticated and permits more flexible operation and easier use.

A cell and battery monitor was also constructed that will work with any cell or battery and with any cycler. This compact monitor operates completely independently from the cycler and interrupts the current if the voltage of the cell or battery violates preset limits. As a result, a cell or battery would be protected from damage in the event of overcharge or overdischarge.

Consideration is being given to a scheme for providing automatic bypass fusing of a battery cell that fails in the open-circuit condition. The fusing would reestablish a current path around the failed cell so that the battery could continue to function at essentially the same voltage, but with one less cell. As a result, the necessity for penetrating the jacket of a high-temperature battery to effect a repair can be eliminated or postponed to a more opportune time. The method promises to be economical and simple, and preliminary work to demonstrate the concept has been started.

3. Battery Testing

(V. M. Kolba, G. W. Redding, E. C. Berrill, J. L. Hamilton)

The purpose of this effort is to evaluate Li-Al/FeS_x cells operated both in series and in parallel arrangements and to compare their performance in batteries with their performance as individual cells. The cells presently under test have been supplied by several commercial fabricators. During this period, a major goal was accomplished, namely, for the first time three Li-Al/FeS cells were operated in a series arrangement. About 95% ampere-hour efficiency and about 80% watt-hour efficiency were achieved. Average specific energy of the three-cell system was about 45 W-hr/kg. Two of the better cells were also operated in series to give an ampere-hour efficiency of 99%, a watt-hour efficiency of 82%, and similar specific energy. A cell equalization system was tested, and a preliminary evaluation of the benefits of equalization indicate a gain of from 14 to 20% in capacity and energy on subsequent cycles.

a. Testing in Parallel and Series Arrangements

Gould Cells. Initial testing of cells interconnected in battery-type arrangements was discussed in ANL-76-35, p. 34. As noted in that report, a modified conditioning procedure was used with FeS_2 Cells 2-004 and 2-005 from Gould Inc. in an effort to avoid problems with high resistance that had been encountered with other Gould cells. After electrolyte-filling, these cells were started up and conditioned individually in the test wells. They were then tested in parallel under deep discharge and short cycle (for 1 hr

at the 2-hr discharge rate and for 1 hr at the 4-hr discharge rate) conditions at 450°C. Results of the tests are given in Table II-8. In series arrangement, Cell 2-004 limited the battery capacity because of a high leakage current. Cell 2-004 was removed from testing and operation of Cell 2-005 was continued as a life test, accumulating ~1740 hr and 141 cycles at a utilization of about 59% and an ampere-hour efficiency of ~99% in Cycle 140 at the 10-hr discharge. After a temperature excursion to ~650°C resulting from a controller malfunction, the utilization decreased to about 19% but the ampere-hour efficiency remained near 100%. After 29 additional cycles, the utilization had decreased to about 17% and the ampere-hour efficiency was still about 98%.

The parallel operation of Cells 2-004 and 2-005 showed that the attainable capacity was less than the sum of the individual capacities, tending toward the lowest capacity cell. Increasing the current from a 6-hr to a 3.6-hr discharge rate reduced the capacity of these cells by about 22% and the energy by about 29%. Under these conditions the ampere-hour and watt-hour efficiencies changed by less than 10% and 15%, respectively.

Testing under short-cycle conditions of 1 hr at the 4-hr discharge rate (20 A) showed that the cells, after reaching equilibrium, provided very reproducible data over 23 cycles, as shown in Table II-9.

Eagle-Picher Cells. To gain insight into the effect of exposure of cells to air, the Eagle-Picher cells were started and conditioned in an inert-atmosphere glove box before being installed in the test wells. (In early tests of Gould cells, there was some concern that the high resistance may have been caused by a slight leakage of the Conax seal which exposed the internal components of the cells to air.)

Testing of the Eagle-Picher FeS cells, as individual cells and in parallel and series arrangements, was begun after the cells had been filled with electrolyte and conditioned, and had undergone qualification testing (see Section II.A.1). After being placed in the test wells, each cell was individually cycled to determine whether its performance had been affected by the freeze-thaw cycle and the subsequent handling in air. A comparison of data from the final cycle of the qualification tests and the initial individual tests in the test wells indicates that a slight decrease (~10%) occurred in the capacity and energy, but the efficiencies remained unchanged.

The cells were connected together in the configurations designated 3P through 6S in Table II-8. These tests showed that cells having similar performance characteristics as individual cells will show similar performances in both series and parallel arrangements. However, in these arrangements, the individual cell voltages must be monitored to prevent charging or discharging a cell beyond the cutoff voltage. When the individual cell voltages are monitored, the first cell reaching the discharge cutoff voltage triggers the charge cycle, and the first cell reaching the charge cutoff voltage triggers either the equalization charge or the next discharge, depending on the mode of operation selected.

b. Equalization Testing

Tests to determine the effects of equalization on the performance of cells in series were conducted in configurations 5S and 6S. After

Table II-8. Summary of Battery Tests

Battery No.[a]	Cells[b]	Discharge Current, A	Peak Capacity, A-hr	Peak Energy, W-hr	Eff., % A-hr	Eff., % W-hr	Cycles	Remarks
2P	2-004,2-005	15	90	121	79	55	8	Deep discharge
		17.5	87	114	73	49	8	Deep discharge
		25	70	86	78	48	2	Deep discharge
		30	15	24	67	43	2	Short cycles, 1 hr at C/2[c] rate
		20	22	30	73	54	27	Short cycles, 1 hr at C/4 rate
2S	2-004,2-005	10	29	73	-	-	3	Limited by 2-004
3P	1B3,1B4	20	133	161	98	81	6	Equalizing charge, 2A; voltage cutoffs based on 1B4
4P	1B3,1B4,1B6	30	136	163	99+	81	7	Limited by 1B3 on discharge
4S	1B3,1B4,1B6	10	40	142	94	82	3	Equalized on each charge; limited by 1B3 on discharge
5S	1B4,1B6	10	67	163	99	~82	4	Limited by 1B4 on discharge
6S	1B4,1B5,1B6	10	76	274	99+	~85	6[d]	Equalized after Cycle 5; limited by 1B5 on discharge

[a] S = series, P = parallel.

[b] Cells 2-004 and 2-005 are Gould FeS_2 cells; 1B3 through 1B6 are Eagle-Picher FeS cells.

[c] Current drawn at a rate that would completely discharge the cell in 2 hr.

[d] Still in operation.

Table II-9. Reproducibility of Test Data over 23 Cycles (cycle conditions: 1 hr at C/4 rate[a])

	Average Value	Standard Deviation
Efficiency, %		
Ampere-hour	69.5	0.61
Watt-hour	51.8	0.37
Average Voltage, V		
Charge	1.9527	0.0015
Discharge	1.4560	0.0014

[a]Current drawn at a rate that would completely discharge the cell in 4 hr.

an equalization cycle, the cells were cycled using a bulk charge only. In this manner of operation, the discharge capacity following the first bulk charge cycle decreased by 10.5% from that of the first discharge cycle after equalization, and decreased by about 19% after the second bulk charge cycle. Similarly, the energy decreased 11 and 20%, respectively. No further reductions took place on subsequent cycling using only bulk charging.

In a second type of test, data from the first discharge cycle after equalization were also compared with those of the preceding discharge cycle without equalization; here, the gain in capacity was 14% and the gain in energy 16%. Results of these two experiments, which show reasonable agreement, indicate that equalization appears to produce gains in capacity and energy of about 14 to 20%. These gains are only temporary, and equalization may be required at the end of every second deep discharge of the battery to attain maximum benefits. The gains in energy are the result of gains in capacity only and not the result of higher average discharge voltage.

c. Battery Heating and Cooling

The temperature changes that occur during cell charging and discharging must be determined so that the heating and cooling requirements for battery design can be established. These temperature changes may influence the nominal operating temperature of the system, which must be controlled to avoid excessive corrosion rates or freezing of the electrolyte. A preliminary experiment to determine gross temperature changes of a cell was conducted in conjunction with a test to determine whether and inert atmosphere is required for short-term cell testing.

A Gould cell (2-006), which had usable capacity of about 23 A-hr early in life, was wrapped in a heater tape (Briskeat) and then in about 12 cm of Kaowool insulation, and placed in a container in an air environment. The cell has now been operated for more than 1200 hr at temperatures from 425 to 475°C. During this period, the usable capacity, which was about 17.5 A-hr after five start-up cycles, increased to about 20 A-hr. The cell temperature, which was monitored during cycling by a thermocouple attached to the outer cell case, varied from 6 to 10°C during a charge/

discharge cycle. Additional testing with an improved experimental set-up is planned to quantify cell-temperature changes during operation in battery arrays.

D. Industrial Contracts
(A. A. Chilenskas)

Commercial development of lithium-aluminum/iron sulfide batteries is being implemented by contracting with industrial firms to (1) develop manufacturing capability for required cell materials, (2) develop manufacturing techniques for electrodes and cells, (3) develop components such as insulated battery casings, electrical feedthroughs, and charging control systems, and (4) fabricate and test hardware.

1. Cell Development and Fabrication
(R. C. Elliott, R. F. Malecha*)

Work is continuing under the contracts made with three firms--Gould Inc., Eagle-Picher Industries, Inc., and Catalyst Research Corp.--to develop manufacturing procedures and fabricate test cells and electrodes. The status of the work under these three contracts is summarized below.

Gould Inc. As reported previously (ANL-76-35, p. 35), the work under the original Gould contract was redirected toward the development and fabrication of cells with uncharged, hot-pressed FeS electrodes. Gould recently completed a large glove-box facility, which will provide the capability for fulfilling their present contract. The new facility was approved by a committee from ANL, as specified in the addendum to the Gould work statement.

As part of the design effort on cells with hot-pressed uncharged FeS electrodes, Gould is using a computer model that takes into account the relevant factors in cell design. The model has been used to establish electrode specifications and to predict performance characteristics.

A review of the proposed designs will be held during the forthcoming quarter.

Eagle-Picher Contract. The cells covered by this contract have cold-pressed positive and negative electrodes and are fabricated in a helium-atmosphere glove box. Four cells (two FeS and two FeS_2) were delivered to ANL in January 1976 and served as "prototypes" for testing before the remainder of the cells were fabricated. As a result of this testing (see Section II.A.1), certain design changes were made that were common to both types of cells and, in the FeS_2 cells, the joint between the positive-electrode current collector and terminal was redesigned. In April 1976, the remaining FeS cells and six of the twelve FeS_2 cells under the contract were delivered. The FeS cells have been tested extensively (see Sections II.A.1 and II.C.3). Testing of the FeS_2 cells with the redesigned terminal connection proceeded to the point where approval was given to Eagle-Picher to fabricate the six remaining FeS_2 cells in this series. Delivery of these cells is expected in August 1976.

In a joint effort, Eagle-Picher and ANL identified a number of design changes, based on operating experience with the present Li-Al/FeS_2

---

*Chemical Engineering Division, ANL.

cells, that are aimed at improving cell specific energy and specific power. The modified designs served as the basis for a proposal by Eagle-Picher for a continuation of their contract. The proposal, which is presently being reviewed by ANL, calls for the fabrication of a total of 58 cells, with separate design modifications to be incorporated in different sets of cells.

Catalyst Research Contract. Because Catalyst Research encountered difficulties in fabricating the cast Li-Al negative electrode for the cells under their contract, ANL requested that the first two cells be made with negative electrodes of Li-Al powder vibratorily loaded in porous structures. This substitution would allow (although at the possible expense of lower specific energy) a more rapid evaluation of the proposed scheme for fabricating the cells in dry air. The cast negative electrodes will be used in later cells.

Catalyst Research has completed the fabrication of the first FeS_2 cell in dry air; the cell has been filled with electrolyte (with some difficulties due to cell gassing), and is now undergoing electrical cycling at their facility.

2. Component Development

a. Electrode Separators
(J. E. Battles)

The development of electrode separators to meet our technical and cost goals is being pursued under R&D contracts as summarized below. Related laboratory work is presented in Section II.B.2 of this report.

The Carborundum Co. Development efforts under the Carborundum contract are concentrated on developing a process for binding BN fibers with BN to obtain a paper or felt separator. Efforts are being continued to define the necessary parameters (preparation, pyrolysis, etc.) to obtain uniform bonding and to control fiber distribution, pore size, porosity and thickness. Discussions are under way for an extension of this contract (4 to 6 months) to allow for completion of these development efforts. Also, a contract is being initiated for the purchase of 600 lb of BN roving in FY 1977 and FY 1978. Carborundum will undertake the design, engineering and construction of a facility to produce 5000-10,000 lb of BN fiber annually.

University of Florida.* Prototype separators of both Y_2O_3 and BN fibers have been prepared using an asbestos fiber (~10 wt %) as a binder to provide the mechanical strength necessary for handling during cell assembly. Samples have been tested in cells with reasonably good results. Efforts are continuing on determining the parameters that control the physical and mechanical properties. Also, efforts are being initiated to make several pilot plant runs on a continuous paper-making machine later this year. This contract has been renewed for an additional 18 months starting April 1, 1976.

Zircar Products, Inc. Prototype yttria felts made by a precursory process have been tested in small cells with good results. Additional materials have been obtained for larger-scale testing. Discussions are under way with Zircar Products, Inc. for an R&D contract for the further development of Y_2O_3 felt, in particular, improvements in mechanical strength, and control

*Contract funded directly by ERDA.

of porosity, pore size, and thickness. Also, effort will be directed toward developing BN felts using the precursory process.

Fiber Materials, Inc. The development contract with Fiber Materials, Inc. became effective in late June 1976. The emphasis in this program is the development of a process for making BN fibers and the evaluation of paper-making concepts using various blends of fiber lengths to improve mechanical properties.

North Carolina State University. An unsolicited proposal from North Carolina State University has been forwarded to ERDA with our recommendation that the R&D contract be funded. The effort would be related to the development of porous, rigid separators, and a major part would be directed toward the determination of impurities in MgO and the concentrations that affect its compatibility with lithium. Magnesium oxide is a low-cost material that should be compatible with lithium, on the basis of thermodynamic data. However, in tests to date, only single-crystal MgO has exhibited the expected compatibility.

b. Feedthroughs
(K. M. Myles)

Design and development of electrical insulators and compact, low-cost electrical feedthroughs is being carried out by a number of contractors. Work on feedthroughs at ANL is presented in Section II.B.1.

National Beryllia. Difficulties have been experienced in fabricating the 3/16-in.-ID BeO insulators for the modified Conax feedthrough and a similar feedthrough redesigned by ANL; moreover the need for larger-sized parts is growing. Accordingly, the previously existing purchase order for BeO insulators was cancelled and a new one was placed for larger parts. A modified, but more expensive, fabrication scheme should provide a reasonable delivery schedule.

Ceramaseal. Prototypes of the ram-type feedthrough were received and evaluated in a simulated test cell. The results were encouraging but, as expected, relatively low cutoff charge potentials were necessary to avoid corrosion of the materials of construction. Less bulky prototypes are currently being fabricated, and if their performance is satisfactory, alternative construction materials will be considered.

ILC Technology. In view of the premature failures of the feedthroughs previously developed for ANL, the direction of future work is being considered jointly by ANL and ILC. ILC plans to submit a proposal in the near future.

Coors Porcelain. A technique whereby an yttria body is cold-pressed and sintered has been developed by Coors. Samples are being evaluated in compatibility tests and have shown excellent corrosion resistance thus far. Coors is proceeding with the nonmetallic brazing of the Y_2O_3 parts to molybdenum.

c. Electrode Materials

Woven aluminum-foil negative electrodes produced by National Standard for use in uncharged cells were found to be very satisfactory in preliminary cell screening tests. Further development will be directed to the reduction of the weight of the copper-wire current collector and to the addition of about 14 at. % lithium to the aluminum.

d. Electrolyte and Active Materials
(Z. Tomczuk)

The fabrication of uncharged Li-Al/FeS_x cells requires an adequate supply of high-purity Li_2S and LiCl-KCl eutectic for contractor use. The sources for these two key cell components were identified previously (see ANL-76-35, p. 37). An agreement has been reached with Lithcoa under which the quality of the LiCl-KCl eutectic will be upgraded by better sampling and handling techniques. The reliability of these improvements will be monitored by chemical analysis for chloride ion and total alkalinity. Visual inspection will continue to be used to maintain the level of free carbon below 25 ppm (higher values produce a discoloration of the electrolyte).

The other key item, Li_2S, has been produced by Foote Mineral in sufficient quantity (100 lb) to satisfy program needs for at least the next six months. At ANL's request, all of this material was sintered at about 900°C to increase its bulk density.

A possible low-cost method for the preparation of Li_2S is currently being investigated by Eagle-Picher. The method involves the high-temperature (700-900°C) reaction of Li_2CO_3 with H_2S. A small batch of this material was tested and found to be of excellent quality; accordingly, an order for 100 lb has been placed with Eagle-Picher.

e. Cell and Battery Charging
(F. Hornstra)

Gulton Industries is constructing two six-cell voltage equalization chargers (one for Li-Al/FeS batteries and the other for Li-Al/FeS_2) of a type suitable for use on electric vehicles. Bench demonstrations of one of the units in June 1976 at Gulton showed that the unit met specifications; delivery of both units is expected in July.

III. CELL CHEMISTRY
(R. K. Steunenberg)

A. Evaluation of Lithium Sulfide
(Z. Tomczuk, A. E. Martin)

Because of the increasing interest in starting cells from the uncharged state, methods for the preparation of Li_2S and evaluation of the product have assumed greater importance. An experimental investigation was conducted to determine whether impurities in Li_2S could be detected by a simple test procedure, consisting of a heat treatment followed by a metallographic examination. Such a procedure would be useful as a routine quality check to identify any off-grade material.

Samples of five lots of Li_2S were sintered at 950 to 1050°C and samples of four of these lots were melted at about 1400°C. The products were examined metallographically. With one exception, no impurities were evident at the grain boundaries of the Li_2S crystals in these heat-treated samples. The atypical result was obtained on a specially selected, impure-appearing portion of one lot. The melted product from this sample contained 20 to 30% of a second-phase impurity, which was subsequently identified as Li_2SiO_3 by X-ray diffraction.* However, a more representative sample of this same lot did not show a second phase after melting. Thus, the above procedure appears to be suitable only for determining gross impurities.

A check was made on the characteristics of Li_2S-Li_2O mixtures to determine why Li_2O, which was expected to be a minor impurity in Li_2S, was not detected by the above tests. Laboratory tests showed that Li_2S and Li_2O form a simple eutectic at 975°C near a 1:1 mole ratio; at the eutectic temperature, Li_2S and Li_2O are essentially insoluble in each other. Thus, one would expect that Li_2O at low concentrations would be evident in metallographic tests. To check this possibility, a sample of Li_2S, to which 1 wt % Li_2O had been added, was heated to 1000°C and then examined metallographically. The Li_2O was clearly visible at the grain boundaries of the Li_2S crystals. This result suggests that less than 1 wt % Li_2O had been present in the five lots of Li_2S that were tested and, consequently, that Li_2O is not a common impurity in the Li_2S received to date.

B. Wetting Characteristics of LiCl-KCl Electrolyte
(J. G. Eberhart)

Efficient operation of a lithium-aluminum/iron sulfide cell requires that the molten LiCl-KCl electrolyte wet the cell separator and particle retainers so that electrolyte can easily pass through these porous materials during discharge and charge of the cells. Measurements have been continued on two aspects of separator and particle retainer wettability: (1) the advancing and receding contact angles of the molten salt on solid surfaces of the materials of interest and (2) the penetrability by molten salt of fabrics, papers, felts, or screens made of these materials.

A new apparatus was constructed for determining advancing and receding contact angles by the tilted-plate method.[2] An existing tube furnace within

*Analyses performed by B. S. Tani of the Analytical Chemistry Laboratory, ANL.

a glovebox was modified for these measurements by mounting a heating stage on a stainless steel rod which is supported at either end of the furnace tube by a steel sleeve. The solid surface to be studied is attached to the heating stage, and the surface is tilted by rotating the rod. When the substrate is sufficiently tilted that a molten-salt drop on its surface is on the verge of rolling off, the advancing and receding contact angles can be observed on the same drop and can be followed as a function of time.

A molten-salt penetration test was performed on yttria felt from Zircar Products, Inc. The felt was 1.0 mm thick and had a weight per unit area of 290 g/m^2. The yttria felt was mounted on the holder and immersed in a 2.54-cm head of high-purity molten LiCl-KCl* at 400°C under 1-atm helium pressure. The holder permitted contact between the salt and felt only on the felt's lower surface. After an initial 1 hr of contact, during which no penetration occurred, the felt was penetrated by the molten salt. Thereafter, the molten salt easily passed through the felt in either direction. This behavior suggests a change in the molten-salt contact angles with time. To verify the hypothesis of time-dependent wettability, contact-angle measurements were made on a sintered plaque of yttria.** The advancing and receding contact angles, θ_A and θ_R, were measured at 375°C in helium at 1 atm pressure. The initial contact angles were $\theta_A = 147°$ and $\theta_R = 74°$; these angles fall in the ranges to be expected for a material that is difficult to penetrate, namely, $\theta_A > 90°$ and $\theta_R < 90°$. Both θ_A and θ_R decreased continuously with time, however, until after 1 hr they had reached steady values of $\theta_A = 90°$ and $\theta_R = 13°$. These final or equilibrium contact angles are characteristic of an easy-to-penetrate material, for which $\theta_A < 90°$ and $\theta_R < 90°$.

Consideration is being given to the use of yttria-magnesia, rather than pure yttria, because of the lower cost of the mixture. To test the molten salt wettability of this material, a sintered plaque of Y_2O_3-50 wt % MgO was prepared.** The contact angles measured were $\theta_A = 102°$ and $\theta_R = 45°$ after a 1-hr equilibration.

Alumina felt was also studied to determine its penetrability by molten salt. The felt, which was in the difficult-to-penetrate category, was penetrated by salt only when the felt was in contact with salt at both surfaces and the system was evacuated and repressurized with helium. The wettability of sintered alumina corroborated this finding. The alumina surface had molten salt contact angles of $\theta_A = 134°$ and $\theta_R = 55°$. The data from the tests performed on yttria, yttria-magnesia, and alumina are summarized in Table III-1, along with previously reported data. It is seen that alumina and boron nitride have essentially the same wetting behavior in the molten salt and are the most difficult to wet of all the materials tested.

C. Electrochemical Studies of Metal Sulfide Phases
(C. G. Cajigas, C. A. Melendres)

Investigations are being undertaken to determine the electrochemical behavior of metal sulfide phases that are formed during the charging and discharging of FeS_x (x = 1 or 2) electrodes. The objective is to obtain

*Purified salt obtained from the Anderson Physics Laboratories, Champaign, Illinois.

**Prepared by W. D. Tuohig of the Materials Development Group.

Table III-1. Wetting and Penetration Properties of Separator and Particle Retainer Materials by Molten Salt[a]

Material	Solid Surface Contact Angles, deg θ_A	θ_R	Penetration Tests Type of Material	Penetration Category
Y_2O_3	90[b]	13[b]	felt	easy[b]
304 SS	93	10	screen	easy
Y_2O_3-MgO	102[b]	45[b]	-	-
ZrO_2	105	45	fabric	easy
graphite	117	55	fabric	difficult
Al_2O_3	134	55	felt	difficult
BN	138	54	fabric	difficult
BN	138	54	paper	difficult

[a]Contact angle measurements were made at 375°C; penetrability determinations were performed at 400°C.

[b]Equilibrium behavior after 1 hr.

thermodynamic data on the formation of these compounds; these data will aid in the engineering design of cells and batteries. Free energies of formation, for example, are directly calculable from measured emfs, while the temperature coefficient of potential should yield the entropy change.

Potentiometric measurements were carried out initially to define the potential-determining reaction for the Fe/FeS electrode. Assuming this system to be an electrode of the second kind, its potential may be expected to depend on the S^{2-} concentration through the Nernst equation

$$E = E^{\circ}_{Fe/Fe^{2+}} + \frac{RT}{nF} 2.3 \log \frac{a_{FeS}}{K_{sp}\, a_{Fe}} - \frac{RT}{nF} 2.3 \log a_{S^{2-}} \qquad (1)$$

where the a's refer to activities (and may be taken as equal to concentration) of the components indicated and K_{sp} is the solubility-product constant of FeS. The emf of the cell

$$LiAl/LiCl\text{-}KCl/Fe,FeS,S^{2-}$$

was measured as a function of S^{2-} concentration, which was varied by the addition of Li_2S. Preliminary results are shown in Fig. III-1 for an initial FeS concentration of 9.1×10^{-6} molal and a temperature of 450°C. It is seen that Nernstian behavior appears to be followed, but the measured value of n (the number of electrons involved in the potential-determining reaction) is 1-1.5, which indicates possibly a more complex set of reactions than the simple two-electron transfer reaction, $Fe + S^{2-} \rightarrow FeS + 2e^{-}$.

Initial measurements of the temperature coefficient of emf for the Fe/FeS couple have been made. The results have been difficult to reproduce and have

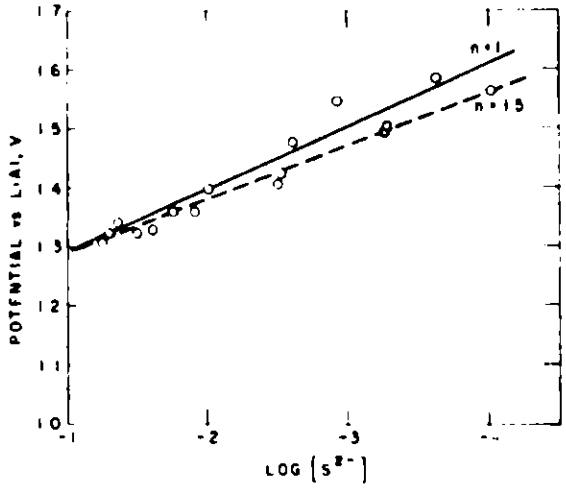

Fig. III-1. Effect of Sulfide Concentration on Fe/FeS Potential

varied from -0.33 to -0.88 mV/°C in the temperature range from 450 to 575°C. In an attempt to obtain better precision, the potentials and temperature coefficients for mixtures of sulfide phases are being measured. Such mixtures will represent the FeS electrode at different states of charge or discharge and hence thermodynamic quantities for the intermediate compounds formed during operation of the electrode may also be obtained.

IV. ADVANCED CELL ENGINEERING
(W. J. Walsh)

The effort in this part of the program is directed primarily toward the development and testing of Li-Al/FeS_x cells having improved performance and/or lower cost. The work, which is presently concentrated on the development of advanced electrodes and cell configurations, complements the effort on commercial development, so that any technical advances can be incorporated as quickly as possible into the cells that are being fabricated by industrial firms. Development work is presently centered on Li-Al/FeS_x cells that are assembled in the uncharged state. In these cells, the positive electrode is initially prepared from a mixture of iron powder, Li_2S, and electrolyte, and the negative electrode consists of a porous aluminum plaque. Upon charging, a lithium-aluminum alloy is formed in the negative electrode, and FeS (or FeS_2, depending on the Fe/Li_2S ratio) in the positive.

A. Uncharged Li-Al/FeS_x Cells

1. Li-Al/FeS Cells
(H. Shimotake, L. G. Bartholme)

The development of uncharged Li-Al/FeS cells has alleviated some major problems that had been previously encountered with FeS-type cells, namely, low utilization of the active material in the positive electrode, and gassing from both electrodes. Moreover, in the present fabrication procedure, the use of sintered Li_2S provides a pressed compact with improved physical characteristics. Several problems remain with the uncharged FeS cells. One is that electrode swelling has not been eliminated, as shown by postoperative examinations of Cells R-7 and R-10 (see Section II.B.4), which were not mechanically restrained. Efforts to alleviate the swelling are being continued. Another problem with the uncharged cells is that between 10 and 20% of the lithium alloyed in the negative electrode after the charge-formation cycles remains in the negative electrode and does not contribute to cell capacity in subsequent discharges. Therefore, several methods of providing additional negative electrode capacity are being investigated.

The addition of Li_2C_2 clearly improved the achievable capacity of Cell R-10 (see ANL-76-35, p. 47). Because of the favorable results achieved with Cell R-10, calcium carbide was added in Cell R-12 with the expectation that extra capacity might be added to the negative electrode by dissociation of the calcium carbide to calcium and carbon and subsequent alloying of the calcium with the Li-Al in the negative electrode, while the carbon would remain in the positive electrode as a conductive material. In Cell R-13, $CaCl_2$ was added to the LiCl-KCl eutectic electrolyte. In small-scale cells, the addition of $CaCl_2$ was beneficial to cell performance, possibly by modifying the J phase* in the positive electrode and thereby increasing utilization. The formation of a Ca-Li-Al alloy in the negative electrode, which was also considered a possibility, might be beneficial through prevention of excessive fragmentation of the Li-Al alloy. The performance results for these two cells showed no significant improvement from the addition of calcium to the systems; however, a check on the possible formation of Ca-Al-Li alloy will be made through postoperative metallographic analyses when operation of the cells is terminated.

*Approximate composition, $Li_{0.4}K_{2.8}Fe_{12}S_{13}$.

An effort to reduce the electrolyte fraction in the uncharged positive electrode was also investigated. In Cell R-14, an electrolyte fraction of ∿18 vol % instead of the usual 45 vol % was used in the hot-pressed positive plaque. The plaque was successfully pressed at 6000 psi instead of the usual 1000 psi. No copper was added to this electrode. The ohmic resistance of the cell was only 3.8 mΩ, the lowest resistance achieved in this type of cell. This extremely low resistance is attributed to good contact between the current collector and the active materials. Typical performance curves of Cell R-14 are shown in Fig. IV-1.

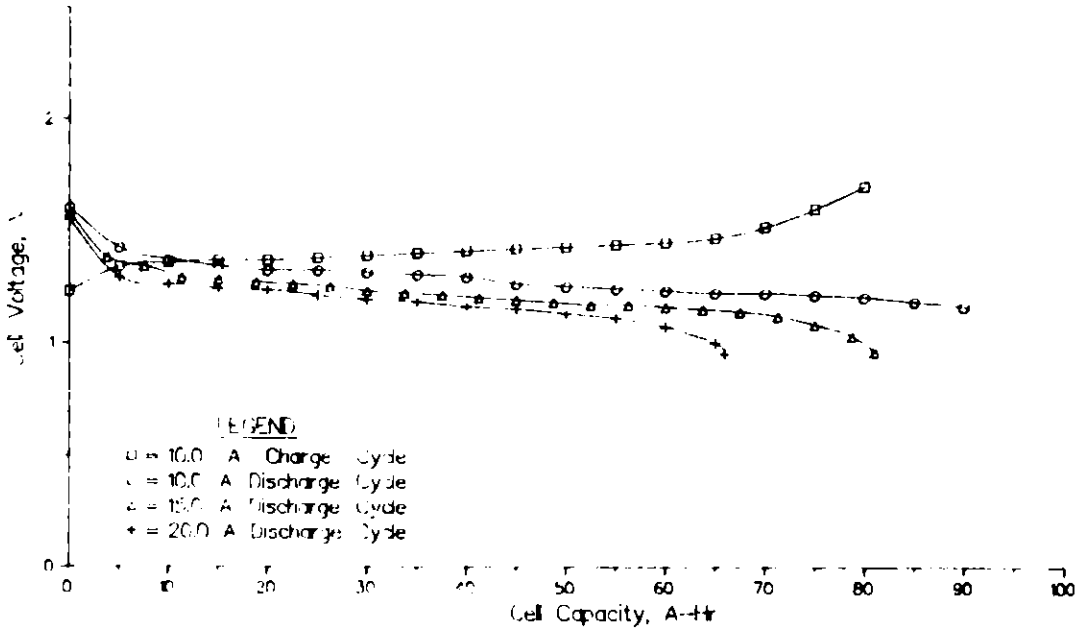

Fig. IV-1. Performance Curves for Cell R-14 (theoretical capacity, 106 A-hr)

2. Li-Al/FeS_2 Cells
(H. Shimotake, L. G. Bartholme, J. D. Arntzen)

Operation of Cell R-8, an uncharged FeS_2 cell described in the preceding report (ANL-76-35, p. 49), is being continued. An accidental freezing, during a recent power failure, and subsequent remelting apparently had no adverse effects on cell performance. After 2974 hr and 400 cycles the performance is stable, although the ampere-hour efficiency is now only ∿61%; this low value indicates a partial but constant short circuit.

Cell R-11 was operated to test Hastelloy B as the current collector in an FeS_2 cell. The cell demonstrated an extremely high utilization (>90% of theoretical) of FeS_2 in the early cycles, as shown in Fig. IV-2. However, after 15 cycles, utilization decreased to ∿50%, and operation of the cell was terminated after 910 hr and 58 cycles.

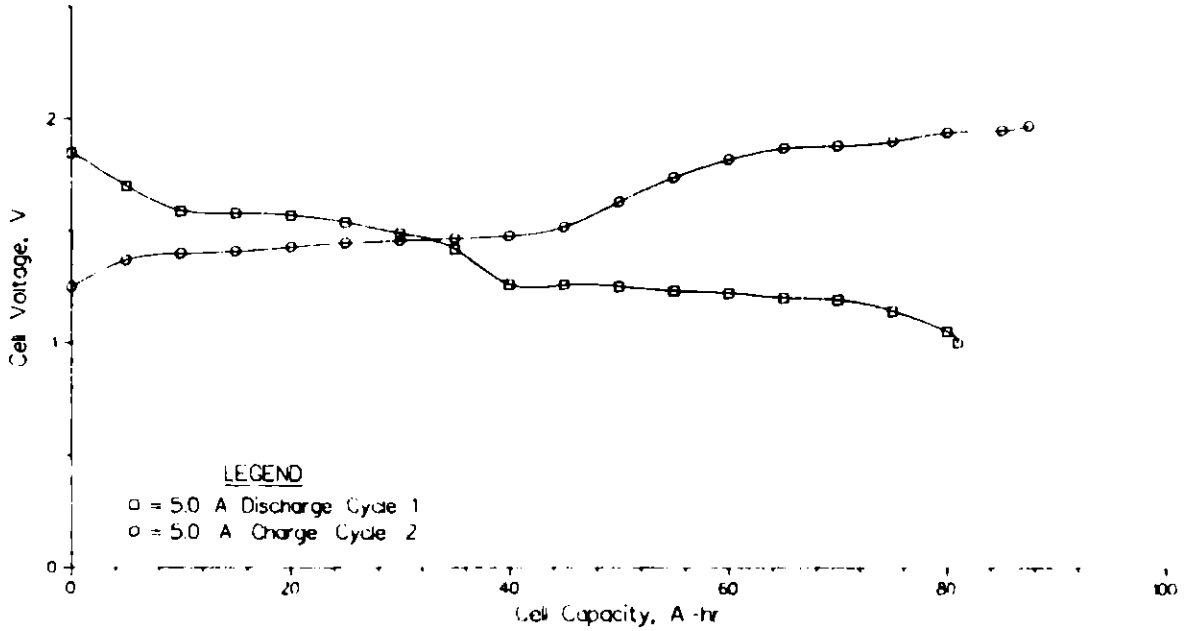

Fig. IV-2. Performance of Cell R-11 during Early Cycles (theoretical capacity, 89 A-hr)

A multiple-electrode, uncharged FeS_2 cell with hot-pressed electrodes is nearing completion. An attempt has been made in the design of this cell to minimize the weight of interior structural components and the inter-electrode distances.

B. Charged Li-Al/FeS Cells
(J. D. Arntzen, K. Gentry,* W. J. Walsh)

Cell BB-1, a prismatic charged FeS cell was tested during this period. Both the positive and negative electrodes in Cell BB-1 were prototype electrodes fabricated by Eagle-Picher Industries, Inc. before delivery of the first electrodes under their contract with ANL. The electrodes were cold-pressed in a dry room (5% relative humidity) and utilized an iron honeycomb current collector structure. The negative electrodes were made from a powdered mixture of Li-Al and LiCl-KCl, and the positive half-electrodes from a mixture of FeS, Cu_2S, and LiCl-KCl.

To form Cell BB-1, the positive electrode halves were assembled back to back and covered with carbon fabric and then with BN fabric. The electrode structure was enclosed in a 5-mil iron "picture frame" and attached to a flexible current lead connector to allow for movement and possible misalignment of the positive electrode and feedthrough. The negative electrodes were enclosed in 325-mesh stainless steel screen envelopes.

Cell BB-1 had a theoretical capacity of 179 A-hr. Typical capacities of the cell were only 70-95 A-hr, however, because of a short circuit that developed in the very early cycles. The performance was very stable throughout

*Industrial participant from Eagle-Picher Industries, Inc.

the life of the cell until it was voluntarily terminated after 3492 hr and 188 cycles. The apparent cause of the short circuit was leakage of the active material from the positive electrode through the corners of the carbon cloth and subsequent penetration of the boron nitride separator fabric. The performance of Cell BB-1 indicates that formation of cold-pressed electrodes in a dry room may be an acceptable procedure.

C. Advanced Cell Designs
(K. E. Anderson, D. R. Vissers, E. C. Gay)

Development work is being carried out on a button cell which may be stacked in a bipolar array. The present cell design utilizes the starved-electrolyte concept as an alternative to the electrolyte-flooded concept. In this cell design, two hot-pressed button electrodes are contained in opposing electrode holders, which are clamped against a boron nitride separator to form the cell, as shown in Fig. IV-3. Potential advantages of the bipolar cell stacks include (1) low fabrication cost, (2) high specific energy, and (3) elimination of the need for feedthroughs.

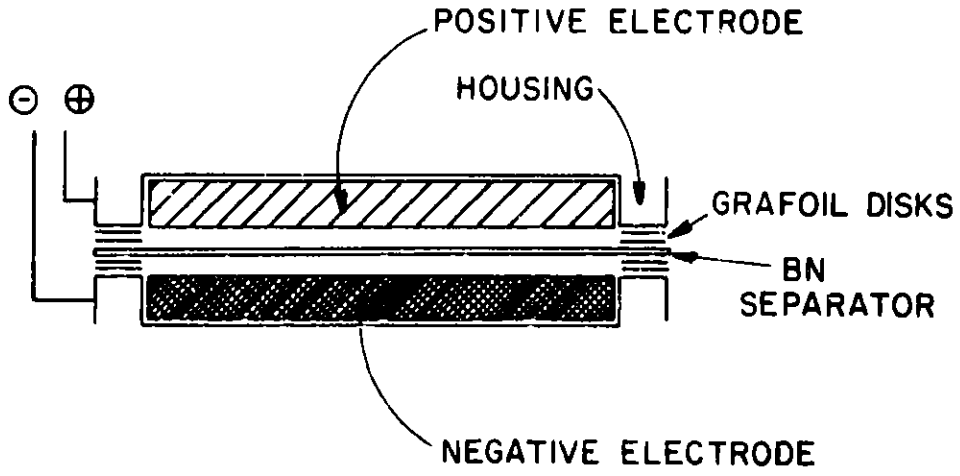

Fig. IV-3. Design of Button Cell

To date, five button type cells have been evaluated: four Li-Al/FeS cells with LiCl-LiF-LiBr electrolyte and one Li-Al/FeS_2 cell with LiCl-KCl electrolyte.

1. FeS Cells

Cell ES-1 was started in the charged state; each electrode contained about 40 vol % electrolyte and had a theoretical capacity of ∿17 A-hr. A 325-mesh stainless steel screen was placed across the face of the FeS electrode to serve as a particle retainer and current collector. The separator was boron nitride fabric wetted with electrolyte. Cell ES-1 was operated at 477°C and a current density of 0.045 A/cm^2; utilization was ∿70% and the ampere-hour efficiency was ∿95%. A typical charge-discharge curve is shown in Fig. IV-4. After approximately 30 cycles the cell shorted; post-operative examination of the cell indicated that particles of Li-Al had penetrated the separator.

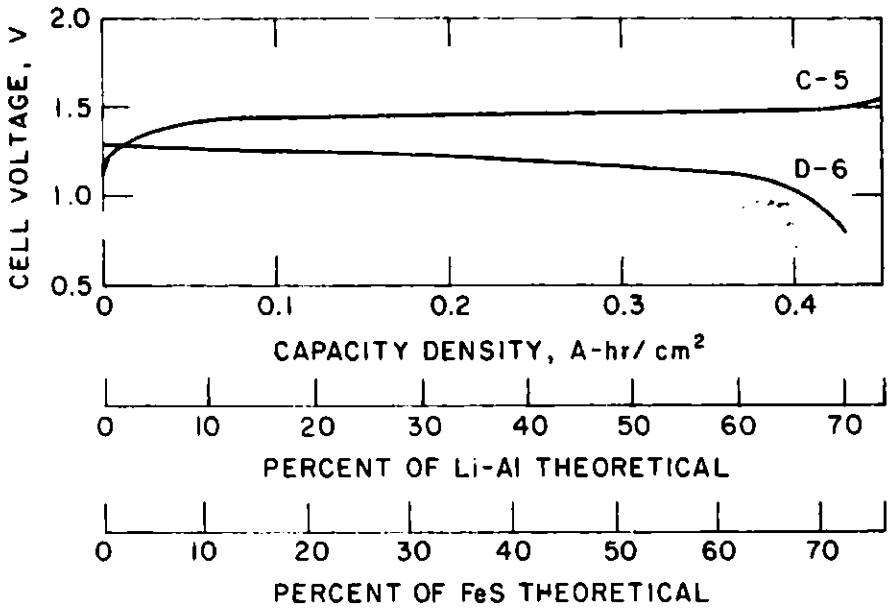

Fig. IV-4. Typical Charge-Discharge Data for Cell ES-1

Cell ES-3 was modified to include a particle retainer of zirconia fabric and a 325-mesh stainless steel screen across the face of each electrode. Cell ES-3 was operated under conditions identical to those of Cell ES-1, and its performance was the same initially, but declined with cycling. After 20 cycles, the utilization had decreased from about 70 to 40% and the ampere-hour efficiency, from about 96 to 80%. Postoperative examination of the cell indicated no evidence of shorting but about 40% of the electrolyte had apparently been lost from the BN separator.

Cells ES-4 and ES-5 were assembled in the uncharged state and copper was added to the positive electrodes in an effort to improve performance. The design of Cell ES-4 was identical to that of Cell ES-3 except that the electrodes were initially uncharged and the cell was sealed at 470°C. Cell ES-4 achieved a utilization of 85% and an ampere-hour efficiency of 99% at a temperature of 470°C and a current density of 0.025 A/cm^2. However, a temperature excursion (from a relay failure) during the 26th cycle appeared to adversely affect the cycle life of the cell. After 56 cycles, utilization had decreased to ~50%, and operation of the cell was terminated. A postoperative examination of the cell indicated no evidence of shorting and a very slight loss of electrolyte from the cell. However, a transfer of electrolyte from the boron nitride separator to the zirconia fabric appeared to have occurred.

In Cell ES-5, the zirconia fabric and stainless steel screens were replaced by a single sheet of porous (5-μm pore size) stainless steel fibers. This sheet was inserted across the face of the negative electrode to reduce electrolyte wicking from the boron nitride fabric. Attempts to operate Cell ES-5 after it had been sealed at 470°C were unsuccessful. A postoperative examination of the cell indicated that the fine fibers from the porous sheet of stainless steel had penetrated the BN separator and shorted the cell. Hence, this material does not appear to be suitable for uses that place it in contact with the electrode separator.

2. FeS_2 Cells

Cell ES-2 was started in the charged state. The positive electrode contained 19.2 A-hr of FeS_2 and 3.4 A-hr of CoS_2, 40 vol % electrolyte, and 30 vol % void, while the negative electrode contained 15.7 A-hr of Li-Al, 40 vol % electrolyte, and 30 vol % void. The design of Cell ES-2 was identical to that of Cell ES-1, except that the positive electrode holder was fabricated from ATJ graphite, and the stainless steel screen in the positive electrode was replaced with a tungsten screen. Cell ES-2 was operated at 450°C and was cycled at a current density of 0.020 A/cm^2. Initially, the lithium utilization was about 35% and the ampere-hour efficiency was 99%. The utilization declined rapidly with cycling; after 20 cycles, it was about 5% and the cell operation was terminated. However, the ampere-hour efficiency of the cell had remained very high throughout the operating period.

Postoperative examination of Cell ES-2 indicated that expansion of the electrodes had compressed the boron nitride separator; the compression probably caused the movement of electrolyte out of the BN. The low lithium utilization of Cell ES-2 suggests that the LiCl-KCl electrolyte does not provide adequate lithium-ion transport in a starved-electrolyte cell.

The tentative conclusions drawn from these five tests and plans for future studies may be summarized as follows. Transport of electrolyte from the boron nitride separator is a major problem that causes a loss of cell capacity with cycling. The general movement of electrolyte and Li-Al particles within the cell also contributes to the loss of capacity. The LiCl-KCl electrolyte does not provide adequate lithium-ion transport in these cells. Porous sheets of stainless steel fiber should not be used in direct contact with separator materials because of potential shorting problems. Future studies will be directed toward controlling the movement of electrolyte within the cell, and investigating FeS_2 cells having an electrolyte of LiF-LiCl-LiBr.

D. Advanced Electrode Development
(D. R. Vissers, W. R. Frost, K. E. Anderson)

Effort is presently being directed toward the development of lithium-aluminum electrodes that can maintain high capacities through hundreds of cycles. It is postulated that the decrease in capacity that occurs with cycling results from morphological changes in the active material, and that the very fine particles so produced create serious electronic conduction problems within the electrode. Several methods of alleviating this problem are being considered: (1) improvement in current collection, (2) improvement in retention of Li-Al particles within the electrode, and (3) control of the particle morphology. Studies of the effects of various metal additives, such as indium and calcium, on the morphology of the Li-Al electrode have just been started and will be reported later. A new type of negative electrode* is being evaluated as part of the effort to improve current collection. This electrode, which is designed for use in uncharged cells, is fabricated from a woven fabric of aluminum ribbon, copper-coated iron wire, and copper ribbon. Performance tests of this electrode in Cell JW-12, described below, are very promising.

*Concept development by K. M. Myles of the Materials Development Group; electrode fabricated by National Standard, see Section II.C.2.

The uncharged electrode of Cell JW-12 consisted of five layers of the aluminum fabric described above (0.89 cm thick) contained in a housing of Type 304 stainless steel. The relatively large quantity of current collector (~35 wt %) could be easily decreased in future electrodes. The Li-Al electrode had an area of 15.6 cm^2, a theoretical capacity density of 0.790 A-hr/cm^2, and an electrolyte volume fraction of 0.46 at full charge. The counter electrode was liquid lithium and the electrolyte was LiCl-KCl eutectic.

The capacity density of the cell was measured at charge current densities of 0.05 and 0.10 A/cm^2 and at discharge current densities of 0.05 to 0.30 A/cm^2. The results, presented in Fig. IV-5, are very encouraging. The performance of this new type of Li-Al electrode is as good as or slightly better than the performance of an electrode with Retimet current collectors (Cell DK-19, ANL 75-36, p. 29).

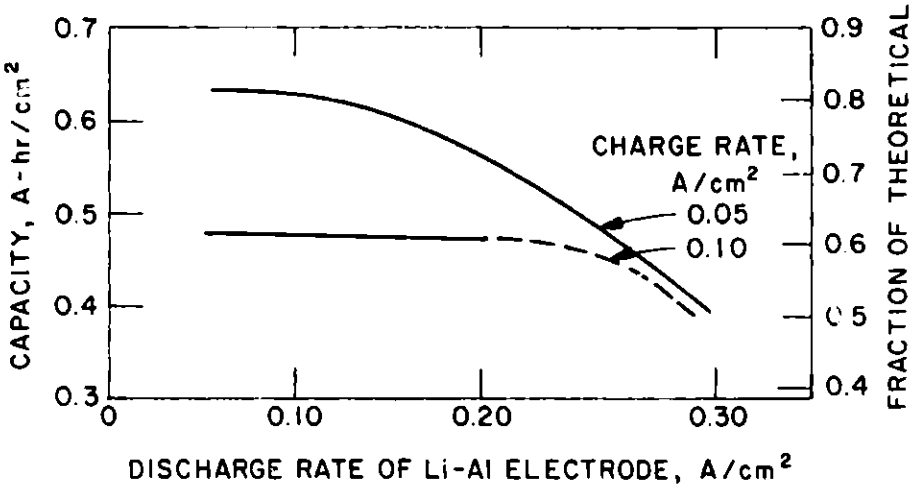

Fig. IV-5. Performance of Cell JW-12

These results are quite important because, for the first time, a wire current collector has been successful in improving the performance of an Li-Al electrode. The results also substantiate a previous postulation that the performance of Li-Al electrodes is limited during discharge by the current-collecting capability of the electrode. The earlier postulation was based on the performance of electrodes of Li-Al powder in Retimet structures. However, the Retimet structure also affected the uniformity of the electrolyte in the electrode, and no definitive conclusions could be drawn.

V. ALTERNATIVE SECONDARY CELL SYSTEMS

(M. F. Roche, H. Shimotake, R. K. Steunenberg, W. J. Walsh)

The objective of this work is the development of new secondary cells, with emphasis being placed on the use of inexpensive, abundant materials; both molten-salt and solid electrolytes are being considered. The experimental work ranges from cyclic voltammetry and preliminary cell tests through construction and operation of engineering-scale, prismatic cells of 100 to 200 A-hr capacity. At present, cells employing various calcium, magnesium, and sodium negative electrodes in combination with iron sulfide positive electrodes are receiving the greatest attention, but tests of other negative- and positive-electrode combinations are also being conducted.

A. Cyclic Voltammetry of Reactive Metals and Their Intermetallic Compounds

(S. J. Preto, M. F. Roche)

Cyclic voltammetry is being used to investigate the electrochemical behavior of candidate electrode materials and to conduct surveys of possible new classes of electrodes for use in molten-salt cells. The molten salts of interest at present are the LiCl-KCl eutectic, LiCl-KCl-$CaCl_2$ mixtures, and the NaCl-$CaCl_2$ eutectic. Calcium and lithium intermetallics with aluminum, magnesium, and Mg_2Si are to be examined. (The lithium study is being done to aid in interpreting the results of the calcium experiments since, in some electrolytes, both Li^+ and Ca^{2+} are expected to interact.) Results of a study of calcium-aluminum and lithium-aluminum compounds are presented here.

The calcium-aluminum compounds were investigated in molten NaCl-$CaCl_2$ eutectic at 550°C. The electrodes of the cyclic-voltammetry cell were as follows:

Reference Electrode. A mixture of FeS and an equivalent amount of its discharge products, CaS and Fe.

Counter Electrode. 20 A-hr of pyrometallurgically prepared $CaAl_2$ powder held in an iron housing of 25-cm^2 area and 1-cm thickness.

Working Electrode. Aluminum foil (22 mA-hr as $CaAl_2$) of 3.1-cm^2 area and 25-μm thickness. Products of foil cycling held in place by iron Retimet and a 325-mesh stainless steel screen.

A cyclic voltammogram for charge and discharge of $CaAl_4$ and $CaAl_2$ is shown in Fig. V-1. The emfs measured at 550°C for the reactions

$$4Al + CaS + Fe \rightarrow CaAl_4 + FeS \quad (1)$$

$$CaAl_4 + CaS + Fe \rightarrow 2CaAl_2 + FeS \quad (2)$$

were 1.171 V and 1.415 V, respectively. The sum of the discharge-peak capacities in Cycle 1, 8.0 mA-hr (for $CaAl_2 \rightarrow CaAl_4$) and 7.8 mA-hr (for $CaAl_4 \rightarrow Al$), was 72% of the theoretical capacity of 22 mA-hr. Cycling of the working electrode led to a decline in its capacity with cycle number as can be seen by comparing Cycle 5 with Cycle 1 in Fig. V-1. The decline seems to be due to mechanical separation of particles that are formed by cycling; tests of methods

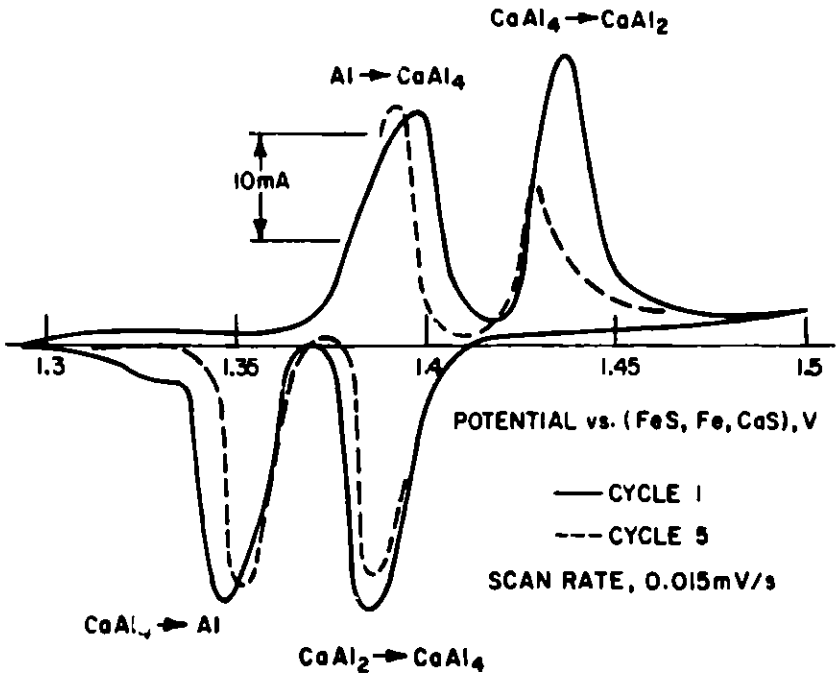

Fig. V-1. Cyclic Voltammogram of Charge and Discharge of $CaAl_4$ and $CaAl_2$ in Molten $CaCl_2$-NaCl Eutectic at 550°C.

to minimize these capacity losses may lead to improved electrodes for conventional cells. In conventional cell studies, reported previously,[3] we were unable to detect these two Ca-Al reactions, and the conclusion was reached that $CaAl_2$ did not form in NaCl-$CaCl_2$ electrolyte. Because of the voltammetry data, we now conclude that both $CaAl_2$ and $CaAl_4$ were being formed in the Ca-Al/FeS cells, but the proximity of the reaction emfs made separation of the plateaus difficult.

In another voltammetry experiment in NaCl-$CaCl_2$ electrolyte, it was found that zirconia fabric, which is used in many cells as a retainer for active materials, is itself electroactive in the presence of calcium ion and cycles without capacity loss. A preliminary interpretation of the rather complex voltammogram is that zirconia is being reduced in stages to a mixture of CaO and zirconium at about 1.25 V *vs.* (FeS, Fe, CaS). Experiments are being done to better define the reaction and to further examine this type of electrode as an alternative to the alloy electrodes.

The β-LiAl compound was investigated in molten LiCl-KCl eutectic at 465°C. The electrodes in this cyclic-voltammetry cell were as follows:

Reference Electrode. LiAl (rod enclosed in boron nitride fabric).

Counter Electrode. 8 A-hr LiAl formed electrochemically from aluminum wire and held in a stainless steel housing of 15-cm^2 area and 0.9-cm^2 thickness.

Working Electrode. Stacked aluminum foils, 195 mg, equivalent to 0.158 A-hr of β-LiAl (45 at. % Li); foils covered by iron Retimet and 325-mesh stainless steel retainers; 3.1-cm^2 area; 0.4-cm thickness.

Voltammograms for cycling of LiAl are shown in Fig. V-2. Peaks are seen for charge and discharge of β-LiAl in the region from 8 to 45 at. % Li and for lithium-rich β-LiAl in the region from 45 to 56 at. % Li. The interpretation given in the figure is based on the Li-Al phase diagram presented in a previous report (Settle and Myles, ANL-76-9, pp. 43-44), and the peak areas are consistent with this interpretation. At low scan rates, 100% utilization of β-LiAl is observed. The utilization decreases at higher rates because charging must be restricted to a narrow voltage range (0 to -300 mV *vs.* LiAl) to avoid formation of liquid lithium.

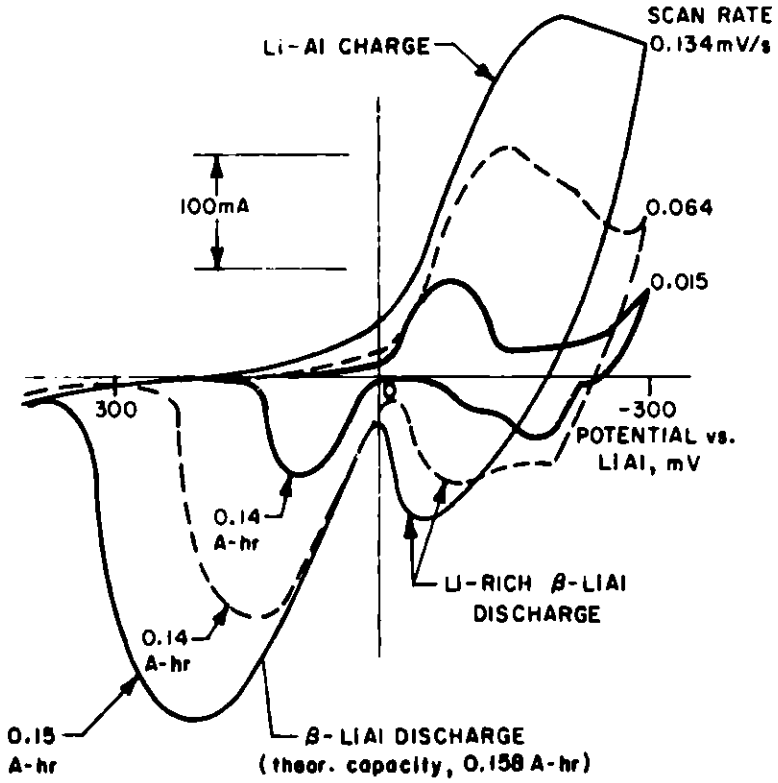

Fig. V-2. Cyclic Voltammograms of LiAl in LiCl-KCl at 465°C

B. Calcium-Electrode Cells
(L. E. Ross, S. J. Preto, A. E. Martin, M. F. Roche)

Two cells employing electrodes of 25-cm^2 area and 0.9-cm thickness were operated to test the effects of variation in electrolyte composition on cell performance. The electrolyte in Cell LR-6 was (in mol %) 38 LiCl-52 KCl-10 $CaCl_2$, and in Cell LP-3 the electrolyte was 54.5 LiCl-14.5 KCl-31 $CaCl_2$. The negative electrodes, which had stainless steel housings with retainers of zirconia fabric and 325-mesh stainless steel screen, were $CaAl_2$ (15 A-hr) for the first 30 to 40 cycles; these were then replaced with 12 A-hr $CaMg_2$ electrodes, which were tested for about 30 cycles. The positive electrodes (FeS, 15 A-hr), which employed iron housings and a combination of zirconia-fabric and iron-screen retainers, were wrapped in BN fabric separators. The cells were contained in stainless steel beakers.

The utilizations of the $CaAl_2$ negative electrodes in both cells ranged from 50% for 10 mA/cm^2 discharges to 25% for 80 mA/cm^2 discharges (charge rates were constant at 10 mA/cm^2). The voltage curves were somewhat flatter for Cell LP-3, which was operated at a higher temperature (500°C *vs.* 460°C for Cell LR-6), and the voltage plateaus corresponding to charge and discharge of $CaAl_4$ and $CaAl_2$ were readily distinguished.

With the $CaMg_2$ negative electrodes, a substantial difference in the performance of the two cells was observed. Figure V-3 illustrates the excellent polarization characteristics of Cell LP-3 and the much poorer characteristics of Cell LR-6. Each polarization curve shown in the figure was obtained by first discharging a portion (stated in the figure caption) of the cell's capacity. The cell was next placed on open circuit for about 10 min, and then successive current densities of 20, 40, 80 and 160 mA/cm2 were applied for 2 min each with an open-circuit relaxation of approximately 5 min between each load. The cell voltage, under load, was recorded at the end of each 2-min application of current, and the data were plotted as shown in the figure. Cell LP-3 was capable of delivering a sustained peak power of about

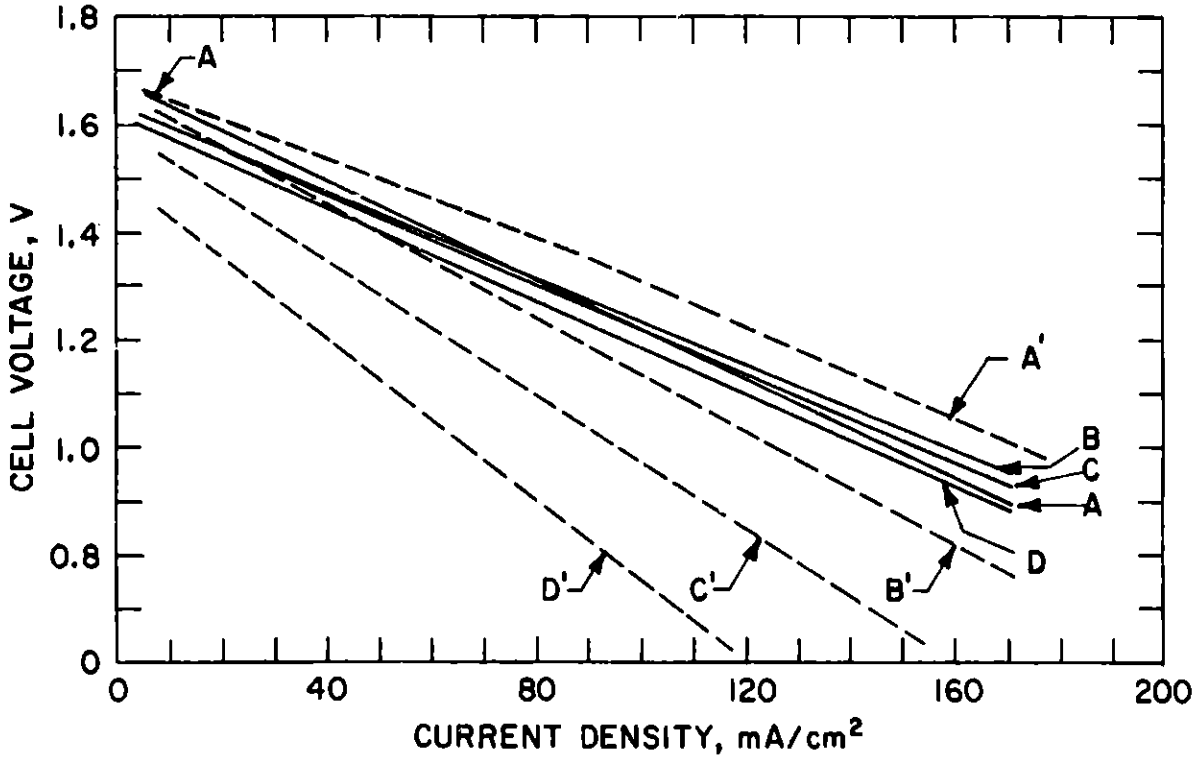

Fig. V-3. Polarization Curves for Cells LP-3 and LR-6 under Two-Minute Current Loads (about 7 A-hr capacities available for both cells at 20 mA/cm^2)

Curves A, A': near full charge
Curves B, B': after 2 A-hr discharge
Curves C, C': after 3.5 A-hr discharge
Curves D, D': after 5.5 A-hr discharge

0.16 W/cm^2 (*i.e.*, 0.8 V • 0.2 A/cm^2) at 80% discharge of its available capacity. These tests demonstrated that, with the use of an appropriate electrolyte (*e.g.*, similar to that in Cell LP-3), high performance can be attained by a cell having a $CaMg_2$ negative electrode and an FeS positive electrode.

C. Preliminary Tests of New Systems
(Z. Tomczuk, A. E. Martin)

Small cells of 0.5 to 1 A-hr capacity are being operated to evaluate the suitability of various electrochemical couples for use in secondary cells. The electrodes have areas of 5 cm^2; the housings of the positive electrodes are graphite (with a porous graphite cover) and those of the negative electrodes are stainless steel.

Two cell systems that were studied briefly were the following: Mg_2Si/KBr-$MgBr_2$ eutectic/FeS_2, which had an emf of 1.391 V at 430°C, and $Mg(Li_2S)$/LiCl-KCl/FeS_2, which had an emf of about 1.5 V at 430°C. Both cells showed poor discharge characteristics and do not appear to merit further study.

A Li-Al/LiCl-KCl/TiS_2 cell, which was operated at 427°C, had an emf of 2.023 V at full charge and gave a utilization of 40% based on formation of $LiTiS_2$. The discharge curves exhibited a gradual decline in voltage with state of discharge and were similar to those reported by Whittingham,[4] who tested ambient-temperature Li/TiS_2 cells in organic electrolytes. Metallographic and X-ray* examinations of the positive-electrode discharge product showed that it consisted of elongated needles of $LiTiS_2$. (The X-ray identification was based on the data of Whittingham.) The TiS_2 positive electrode does not appear to offer any advantages over FeS_2 in molten-salt cells.

A Na/LiCl-NaCl-KCl/FeS_2 cell, which was operated at 420°C and had an emf of 1.545 V, performed very well. The composition of the electrolyte was 10 mol % NaCl in LiCl-KCl eutectic. The liquid sodium electrode was prepared by absorbing an excess of sodium into a porous mat of stainless steel. After fifty cycles, no dewetting of the sodium from the negative electrode structure was observed, the A-hr efficiency was close to 100%, and the cell continued to give full utilization (0.5 A-hr) of the FeS_2 at 20 mA/cm^2. It was assumed that full utilization corresponded to discharge of FeS_2 to Na_2S + FeS (or an equivalent Na-Fe-S compound such as Na_2FeS_2); the cell emf was in good agreement with the value (1.55 V) for the formation of Na_2S + FeS calculated from thermodynamic data.[5] The discharge plateau was very flat, and an attempt to discharge beyond the composition Na_2FeS_2 was unsuccessful. This Na/FeS_2 cell, which has a theoretical specific energy of 500 W-hr/kg, appears to merit further study.

D. Prismatic Cells
(H. Shimotake, W. A. Kremsner)

Engineering studies have been directed toward the development of both positive (FeS) and negative ($CaAl_2$ or $CaMg_2$) electrodes that meet certain performance and cycle life requirements for prismatic cells. Emphasis has been placed on the development of electrodes that appear to be capable of delivering high utilization and long lifetime.

*X-ray examination conducted by B. S. Tani, Analytical Chemistry Laboratory, ANL.

In earlier prismatic cells, which were discussed in the preceding quarterly report (ANL-76-35, p. 56), a mixture of positive material and electrolyte was hot pressed on an iron-mesh current collector while negative material (in the form of a powder) was vibratorily loaded into a porous metal structure. Since that time, several modifications of this design have improved the performance of the cell: (1) the electrode structure was compartmentalized by use of a metal honeycomb structure to prevent settling of active material, and (2) the electrode-structure surface was sealed by porous stainless steel (Dynalloy X7, Fluid Dynamics, Inc., Morristown, N.J.) to prevent possible migration of particulate active materials. At present, an engineering-size cell (12.7 by 12.7 by 3 cm) is being fabricated using the improved design.

Cells that were operated to evaluate new electrode designs and configurations were Cells CA-2, -3, -4, and -5. Cell CA-2, an uncharged, 60 A-hr $CaAl_2$/Fe(Cu)S cell having five electrode plates (two positives and three negatives), was operated to test a multiplate cell with electrodes of conventional design. The cell operated smoothly at 450°C for more than 1000 hr and 66 cycles. The specific energy of this cell was limited to about 35 W-hr/kg because of problems associated with electrode mismatching. The cell was voluntarily terminated; a post-test examination showed settling of negative-electrode material and disintegration of the zirconia fabric retainer, but only limited corrosion of the current collectors.

Cells CA-3 (30 A-hr) and CA-4 (20 A-hr), which were uncharged CaAl/Fe(Cu)S cells with one positive and two negative electrodes, were operated to determine whether a honeycomb electrode structure would prevent settling of active material. In Cell CA-3, a honeycomb structure was used in the positive electrode, and 325-mesh stainless steel screen was employed as a particle retainer in the negative electrode. The positive-electrode particle retainer was zirconia fabric. In Cell CA-4, porous stainless steel sheets were used for particle retention and honeycomb structures were employed in both electrodes. The use of both the honeycomb structure and the porous stainless steel plaques improved cell performance and stability, and prevented capacity decline, but the cell developed a short because of negative-electrode material leakage around the edge of the retainer sheet.

Cell CA-5, a 25 A-hr $CaAl_2$/Fe(Cu)S cell having a design similar to that of Cell CA-4 but with an improved method of welding the retainer, was operated to further test a cell in which both positive and negative electrodes were built using the honeycomb structure and porous stainless steel plaques. From the typical performance of the cell at 500°C, presented in Fig. V-4, and the cell weight (about 350 g), a specific energy of 45 W-hr/kg was calculated for the 7-hr rate. Higher-capacity cells that incorporate the new design features will be operated to determine whether higher specific energy can be realized in larger-scale cells. The goal is a specific energy exceeding 100 W-hr/kg in cells of 100 to 200 A-hr capacity.

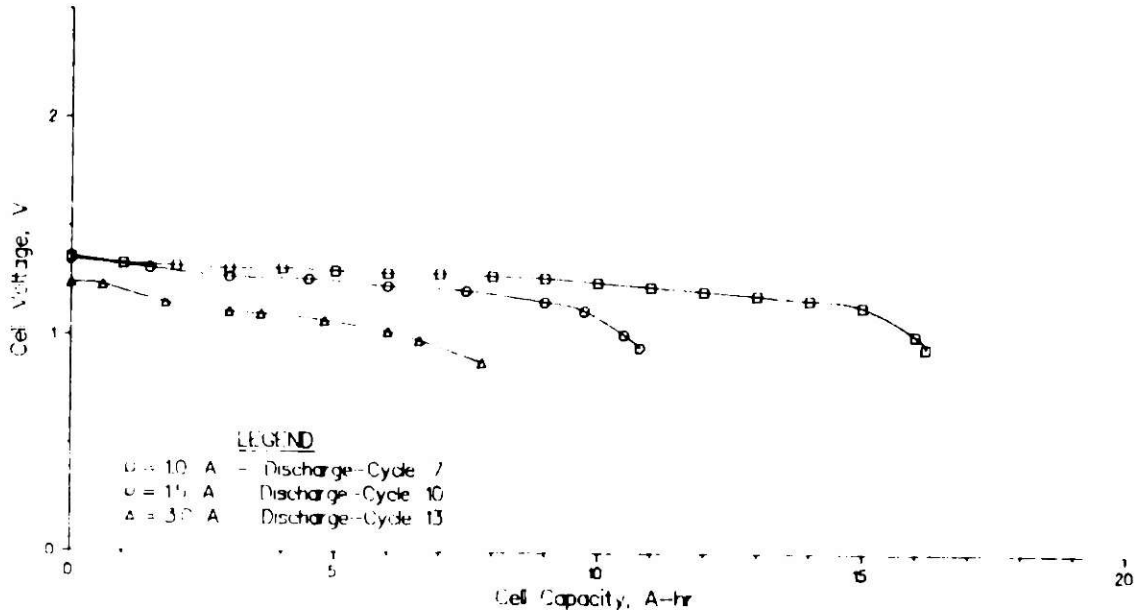

Fig. V-4. Typical Voltage-*vs.*-Capacity Data for Cell CA-5 (theoretical capacity, 25 A-hr)

REFERENCES

1. H. Shimotake and L. G. Bartholme, *Proc. Symp. and Workshop on Advanced Battery Research and Design*, ANL-76-8, p. B-210, Argonne National Laboratory (1976).

2. G. Macdougall and C. Ockrent, Proc. Roy. Soc. (London) *A180*, 151 (1942).

3. S. J. Preto, L. E. Ross, A. E. Martin, and M. F. Roche, *Proc. Symp. and Workshop on Advanced Battery Research and Design*, ANL-76-8, p. B-138, Argonne National Laboratory (1976).

4. M. S. Whittingham, J. Electrochem. Soc. *123*, 315 (1976).

5. J. F. Elliot and M. Gleisner, *Thermochemistry for Steelmaking*, Vol. I, Addison-Wesley Publ. Co., Inc., Reading, Mass. (1960).